Monitoring of the ERS-2 Radar Altimeter range measurement stability

Contract no. 12771/98/I/WE

Final Report

March 1999

P Moore*, MD Reynolds and R J Walmsley
Aston Space Geodesy Group
Division of Civil Engineering
Aston University
Birmingham, B4 7ET
UK

Contact P Moore

*Now at Department of Geomatics
University of Newcastle-upon-Tyne
Newcastle
NE1 7RU
UK

Tel: +44 (0)191 222 5040
Fax: +44 (0)191 222 8691
Email: Philip.Moore@ncl.ac.uk

- **Statement of Work**

It has been established through preliminary studies that ERS-2 Radar Altimeter (RA) presents an unexpected behaviour for what concerns the altimetric range when compared to other altimetric data (ERS-1 or TOPEX/Poseidon) or tide gauge data. First results have shown that the Radar Altimeter on board ERS-2 might drift by few millimetres per year.

In order to ensure the quality of the ERS-2 RA mission over its lifetime, a monitoring of the range measurement stability has to be performed. The aim of this study is to detect and quantify any anomaly (bias, drift, ...) observed on the RA altimetric range since the beginning of the mission by comparison with external data, as TOPEX/Poseidon and tide gauge data. As a result, knowing the size of the problem, such a study will allow to direct the investigations at the instrument level. On the other hand, it could also provide the user community with a correction file in order to enhance the quality of the ERS altimetric data.

Work Description

It is proposed to define the support activities which are the subject of the present Statement of Work into the following:

- Investigation of dual crossovers with TOPEX/Poseidon for long-wavelength spatial variations.
- Comparison of the ERS-2 altimetric data against tide gauge data for precise altimetric range stability analysis**.**

Monitoring of the ERS-2 Radar Altimeter
range measurement stability

1. Introduction

Earlier studies have established that the ERS-2 radar altimeter exhibits unexpected behaviour when compared against contemporaneous altimetry from ERS-1 and TOPEX/Poseidon. First results showed that the ERS-2 radar altimeter might drift at a secular rate exceeding a few millimetres per annum. The objective of this study as formulated in the *Statement of Work* was to monitor the ERS-2 altimetric range measurement over the 30 cycles or so of the first 3 years of the satellite's operation. The *Work Description* outlined two methodologies for detecting and quantifying any anomalous behaviour; namely comparisons against TOPEX/Poseidon and in situ data. The first procedure involves investigation of dual crossovers with TOPEX/Poseidon for long-wavelength spatial behaviour with the second a direct comparison against tide gauge data. This report summarises these procedures, derives time series for the ERS-2 anomalous behaviour and reconciles the results from the different methodologies.

2. Summary of early evidence for anomalous behaviour in ERS-2 altimetry.

From May 1995 to June 1996 the user community had access to altimetry from three contemporaneous missions ERS-1, ERS-2 and TOPEX/Poseidon. ERS-1 was launched in 1991 into a sun-synchronous orbit of inclination 98.53° and altitude near 780 km and has been manoeuvred into several distinct orbits with repeat pass periods of 3, 35, and 168 days. In March 1995, ERS-1 was returned to its 35 day orbit for the so-called second multidisciplinary phase in readiness for the launch of ERS-2 into a similar orbit. After launch in April 1995, ERS-2 was placed into a near identical orbit such that from May 1995 to June 1996 both ERS satellites followed the same ground track but with ERS-2 one day behind ERS-1. The NASA/CNES altimetric satellite TOPEX/Poseidon (T/P) was launched in 1992 into an orbit of inclination 66.06°, altitude near 1336 km and a repeat period of 9.9156 days. T/P carries two altimeters the NASA radar altimeter (NRA) and the CNES solid-state altimeter (SSALT) both of which share a common altimeter. By pre launch agreement the NRA operates for 90% of the time with SSALT filling the remaining 10%.

The tandem operation of ERS-1 and ERS-2 enabled ERS altimetry to be compared at common ground track locations facilitating an inter-calibration of the two satellites. Studies of this type, as well as comparable inter-calibrations against TOPEX/Poseidon, gave the first indications that the ERS-2 altimetric range exhibited anomalous signatures. Unfortunately ERS-1 was deactivated in June 1996 which prevented further direct comparisons of the ERS satellites.

Moore et al (1999) undertook a comparison of ERS-1, ERS-2 and TOPEX (NRA) altimetry during the tandem period. In particular, altimetric range residuals were derived at every 0.25° of latitude by removing the mean sea-level height along the satellite groundtracks. Global ocean variability was then determined at daily intervals over 2° lat. by 3° long. blocks. For the period May 1995 to June 1996 the derived global variability is naturally dominated by the annual signal due to seasonal heating of the oceans - the steric effect. Unfortunately, it is not possible to determine a secular trend as well as the annual signal so simple linear regression was used between 60°N and 60°S. This yielded a 'mean sea-level change' of -4.7±1.5 mm/yr for ERS-1, -5.6±1.3 mm/yr for TOPEX but +9.0±2.1 mm/yr from ERS-2. Although this trend cannot be interpreted as true mean sea-level change due to the dominant annual signal the systematic difference of 14 mm/yr between ERS-2 and both ERS-1 and TOPEX pointed to a clear anomaly with ERS-2.

These studies during the tandem period permit some further deductions as the two ERS satellites are effectively identical and in the same orbit. Hence, any correction that is satellite independent, i.e. common to both satellites, can be excluded. For example, orbit error, although important for many applications, is common to both satellites but can be excluded as repeat pass data eliminates most gravity field error; furthermore the orbits used were derived with common software. The latter would also seem to exclude all modelled geophysical corrections. We are thus looking for a satellite specific cause with the most likely candidates being the altimeter or radiometer performance, the latter supplying the important wet tropospheric altimetric correction. A check has been made (Moore et al, 1999) on the radiometer performance by comparing the ERS radiometric wet tropospheric corrections against the modelled corrections on the ERS altimeter CD ROMs. Comparison of the ratio of radiometric to observed corrections for ERS-1 and ERS-2 do not reveal any significant differences and the difference between the two ratios does not depart significantly from zero. This does not prove that the radiometers perform identically but that the 14 mm/yr secular trend is an order of magnitude larger than any likely difference. Similarly, attempts to model the satellite specific sea-state bias correction had negligible impact. We are thus left with the altimeter itself as the likely cause of the anomalous behaviour. It is beyond the capability of all but a few groups to investigate the altimeter wave form so this study starts from the released ERS data augmented with additional corrections such as the ultra stable oscillator drift and the so-called SPTR corrections. The latter are a prime candidate for the anomalous behaviour particularly as ERS-2 has larger corrections than ERS-1.

Further evidence for identifying the SPTR as likely cause is given in Moore et al (1999). ERS-1 and ERS-2 residuals at the same geographical location but differing in epoch by one day were differenced to obtain a set of repeat pass difference residuals. These differences were combined into daily averages giving the relative bias between ERS-1 and ERS-2 in Figure 1. Also, plotted are the epochs of the so-called SPTR events (see below). It is evident that many of the SPTR epochs correspond to discontinuities.

These and other studies alerted the scientific community to deficiencies with ERS-2 and the need for continuous monitoring of the altimetric range stability. However, with ERS-1 deactivated in 1996 the means to do this are limited to inter-calibrations with TOPEX/Poseidon and comparisons against variability as recorded by the global network of tide gauges. Both methodologies have inherent limitations. For example, TOPEX altimetry itself is not infallible and any drift or signature in the NRA data can be aliased into the ERS-2 result. Care must also be exercised with tide gauge data. In particular it is crucial to ensure that the variability as recorded by continental or island tide gauges is compatible with altimetry over the open seas. Also, local land movement can impose an additional trend upon the oceanographic signal.

Although the study is directed towards ERS-2 most of the analysis is repeated for ERS-1 from April 1992 - June 1996. The use of the two satellites gives confidence to the methodologies and also enables us to investigate differences between the two data sets and to quantify the respective solutions.

A brief summary of the content of the report is now given. Section 3 describes the altimetric data sets and associated corrections. The ERS orbital height as derived at Aston is summarised in section 4. TOPEX data is used in section 5 to validate the global network of tide gauges and to identify a subset where the local signal is representative of that in the open ocean. In section 6, this subset of gauges is used to monitor the TOPEX altimetric range. Dual crossovers between TOPEX and ERS corrected for the TOPEX altimetric range signature are analysed in section 7 for the ERS-2 range anomaly. In section 8, we return to the tide gauge data and recover an alternative time series for the ERS-2 range anomaly through a method reminiscent of that used for TOPEX. The ERS-2 results are compared in section 9 followed by comments and conclusions in the final section.

Figure 1. ERS-1 - ERS-2 daily relative range bias recovered from repeat pass differences.

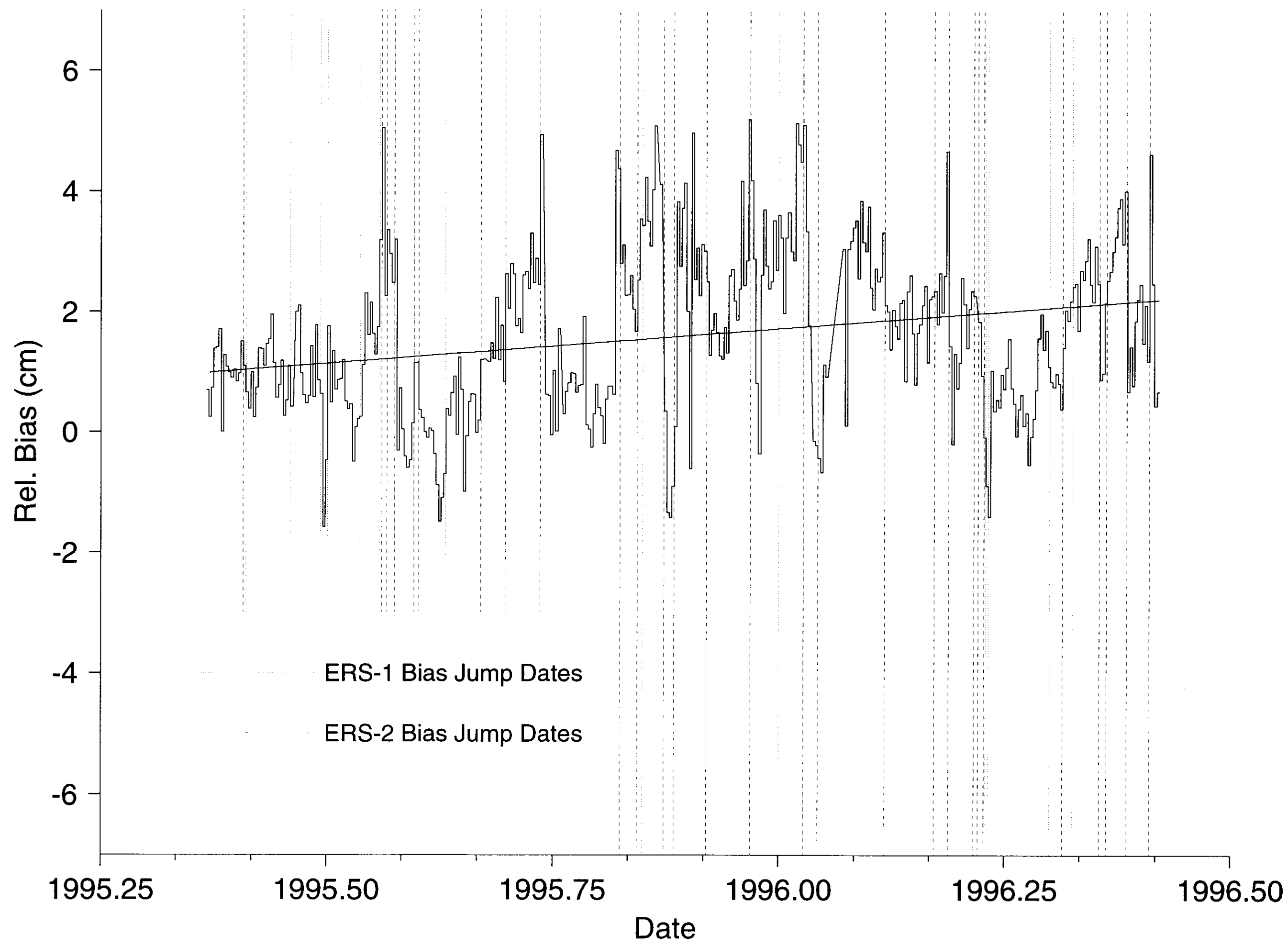

3. Altimetric Data Sets

The corrected altimetric measurement, h^{alt}, of the instantaneous sea-surface height is related to the raw measurement, h^{raw} , by

$$h^{alt} = h^{raw} + h^{se} + h^{tide} + h^{ion} + h^{wet} + h^{dry} + h^{inst} + h^{ssb} \qquad (1)$$

where in brief

h^{raw}	=	altitude corrected for instrumental effects
h^{se}	=	solid Earth tide correction
h^{tide}	=	ocean tide correction including the loading tide
h^{ion}	=	ionospheric correction
h^{wet}	=	wet tropospheric correction
h^{dry}	=	dry tropospheric correction
h^{inst}	=	additional instrumental effects not included in h^{raw} e.g. ultra-stable oscillator bias and bias jumps for ERS
h^{ssb}	=	sea-state bias, a composite of the tracker bias and electromagnetic bias

For most applications an independent estimation of the orbital height above some reference surface is required. This is supplied by orbit determinations based on all available tracking data and gives a height h^{orb} above a reference ellipsoid. The difference

$$h^{orb} - h^{alt} \approx h^{geoid} + h^{ssv} + h^{tt} - h^{bias} \qquad (2)$$

where

h^{geoid}	=	geoid (or mean sea-level) height above the reference surface
h^{ssv}	=	sea-surface variability due to steric heating, ocean currents, atmospheric forcing etc.
h^{tt}	=	time tag bias
h^{bias}	=	residual bias in the range measurement (the objective of this study) including the so-called electronic bias.

Despite the production of global maps of mean sea-level heights from satellite altimetry h^{geoid} is still not known to sufficient accuracy for most purposes. However, advantage can be taken of altimetric measurements at common points on the repeat satellite ground track where the geoid height can be assumed invariant over all cycles. Thus, at such a repeat pass point, the geoid height is common to all data and eliminated by differencing the measurements. In this way the mean sea-level uncertainty is removed and the differenced measurements can be used for ocean variability studies, for example. Alternatively, one may use crossover points at the intersection of an ascending track and a descending track. Again, the geoid height is common and removed in forming the crossover measurements. This principle can be extended to two satellites in different orbits to form a dual crossover. Of course if the two satellites have identical ground tracks (as ERS-1 and ERS-2) then we can form dual repeat pass data as an obvious extension to single satellite repeat pass data. Within this study we concentrate on repeat pass and dual crossover data where the ocean variability h^{ssv} is either assumed negligible - if the two dates (epochs) of the altimetric data are almost the same - or replaced by the variability recorded by a nearby tide gauge.

Within the context of this study a DXO residual at the intersection of the satellite ground tracks is defined by

$$\Delta_{DXO}(t_1, t_2) = (h^{alt}_{T/P}(t_1) - h^{orb}_{T/P}(t_1)) - (h^{alt}_{ERS}(t_2) - h^{orb}_{ERS}(t_2)) \quad (3)$$

where h^{alt} is the altimetric height corrected for all geophysical effects; h^{orb} the corresponding calculated height from the orbit determination for the given satellite and t_1, t_2 the epochs of the T/P and ERS altimetric measurements respectively. On using Equations 1 and 2

$$\begin{aligned}\Delta_{DXO} = {} & (h^{ssv}_{ERS}(t_2) - h^{ssv}_{T/P}(t_1)) + (h^{tt}_{ERS}(t_2) - h^{tt}_{T/P}(t_1)) - \\ & - (h^{bias}_{ERS}(t_2) - h^{bias}_{T/P}(t_1)) + \Delta^{dxo} \end{aligned} \quad (4)$$

where Δ^{dxo} is a term including all other errors eg orbits.

A single satellite crossover (SXO) residual for ERS for example can de deduced from Equation (4) by replacing T/P by ERS, i.e.

$$\begin{aligned}\Delta_{SXO} = {} & (h^{ssv}_{ERS}(t_2) - h^{ssv}_{ERS}(t_1)) + (h^{tt}_{ERS}(t_2) - h^{tt}_{ERS}(t_1)) - \\ & - (h^{bias}_{ERS}(t_2) - h^{bias}_{ERS}(t_1)) + \Delta^{sxo} \end{aligned} \quad (5)$$

Given the nature of the study it is important to state unambiguously the altimetric data, geophysical corrections and orbital positioning employed.

For ERS the altimetric range and most corrections were taken from the Precise Ocean Product (OPR) as issued by CERSAT in the form of CD ROMs. The OPR for ERS-1 was released as distinct versions namely 3.0 - 3.5, 5 and 6.2 - 6.3. Version 5 was an intermediate release between versions 3 and 6 and has not been used in this report. We note here that the CERSAT documents state the equivalence of versions 3.0 - 3.5 but that version 6 utilised different processing procedures and is incompatible with the earlier versions. Version 6 was introduced for the ERS tandem phase. Thus all ERS-2 altimetry and ERS-1 altimetry during the second multidisciplinary phase are versions 6.2 - 6.4.

The ERS OPR altimetry was utilised with the following modifications and choice of corrections:

- DPAF orbital height on the CD ROM was replace by an in-house orbit computation as summarised in the next section.
- Radiometric wet tropospheric correction was applied. Observations were rejected if the radiometic correction was unavailable.

- ERS-2 radiometric wet tropospheric correction was recomputed after pass 650 of cycle 12 (as recommended by CERSAT in the documents accompanying the CD ROM).
- ERS-1 radiometric wet tropospheric correction was corrected for version 3 data as $\Delta h_{corr} = 0.81212\ \Delta h - 1.9256$ (cm) where Δh is the correction given in the OPR (as recommended by CERSAT).
- CSR 3.0 ocean tide computed for ERS-1. Standard for ERS-2
- Pole tide applied.
- Sea-state bias: OPR sea-state bias replaced by -0.0595 swh (significant wave height) for ERS-1 version 3 and by the Gaspar and Ogor 4 parameter sea-state bias corrections for version 6 (as recommended by CERSAT). The value 5.95% (Carnochan, 1997) of swh differs marginally from the CERSAT recommended value of 5.5%.
- Inverse barometric correction applied for dual crossover data but not added for comparison with tide gauges.
- ESRIN correction for the Ultra Stable Oscillator (USO) bias drift was applied.
- ESRIN corrections for ERS bias jumps as characterised by the Single Point Target Response (SPTR) were applied.

Again to avoid any misinterpretation the final two corrections were *added* to the range measurement.

The ERS bias jumps occur when the altimeter is placed in its safe-mode and then reactivated at a later date. The temperature differential over the stand-by period leads to a discontinuity or jump in the range measurement as the clock stabilises to a different temperature regime. According to the Roca and Francis study (1996) the SPTR can quantify the error enabling a correction to the range data to be released by ESRIN. Plots of the ERS corrections for the USO drift and the SPTR jumps are given as Figures 2-5.

For TOPEX the altimetric height, geophysical corrections and orbital height were taken from the AVISO CD ROMs, version C. In particular, we used the

- NASA orbital height.
- TOPEX Microwave Radiometer wet tropospheric correction.

Also, it is important to note that

- Version C is corrected at source for the USO bias drift and the Wallops Flight Center internal correction.
- TOPEX (NRA) and Poseidon (SSALT) were flagged with the latter rejected in most applications.

Poseidon data was retained but flagged and rejected in most applications. This was considered prudent as TOPEX and Poseidon have different characteristics with a small relative altimeter bias and any error in the a priori value will be aliased, for example, into the ERS dual crossover solution. Poseidon is only operational for about one cycle in 10 and its rejection has little overall effect.

TOPEX altimetry has been subjected to intensive examination with a drift of -2.3±1.2 mm/yr determined (Nerem et al, 1997) by comparison against tide gauge data. Most of this is attributable to a corresponding drift in the TOPEX Microwave Radiometer (TMR). For example, a TMR drift of -1.2±0.4 mm/yr was estimated by Haines and Bar-Sever (1998) by comparison against terrestrial GPS receivers. No correction has been applied for this drift as it is estimated in section 6.

Figure 2. ERS-1 Ultra Stable Oscillator (USO) corrections (as supplied by ESRIN)

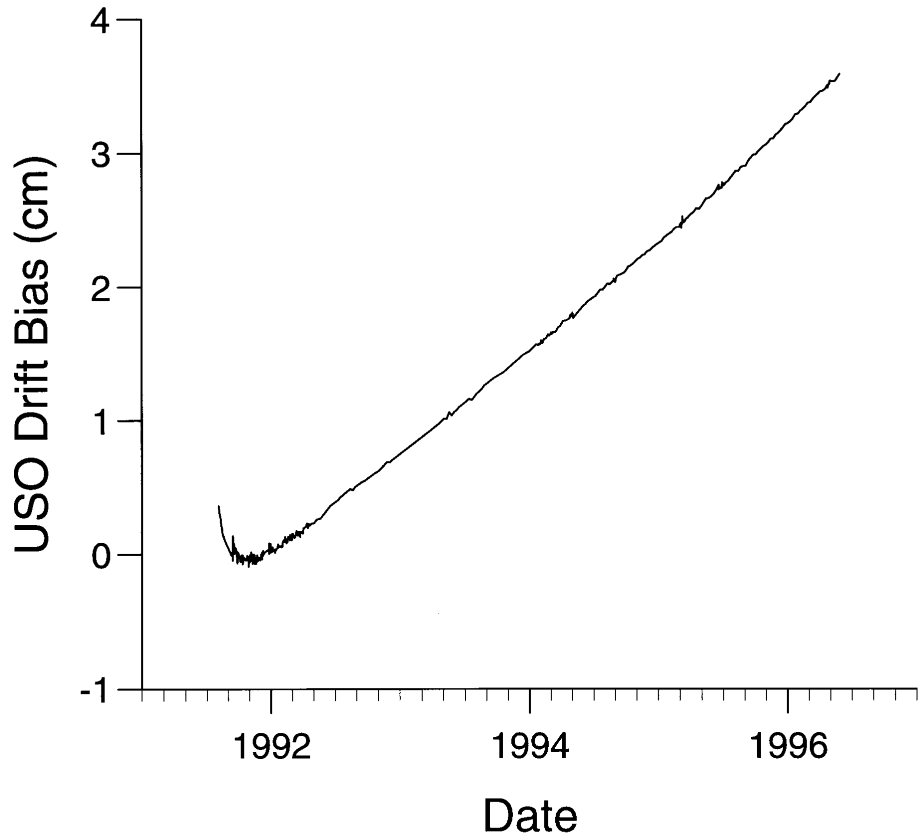

Figure 3. ERS−1 bias jumps as characterised by SPTR

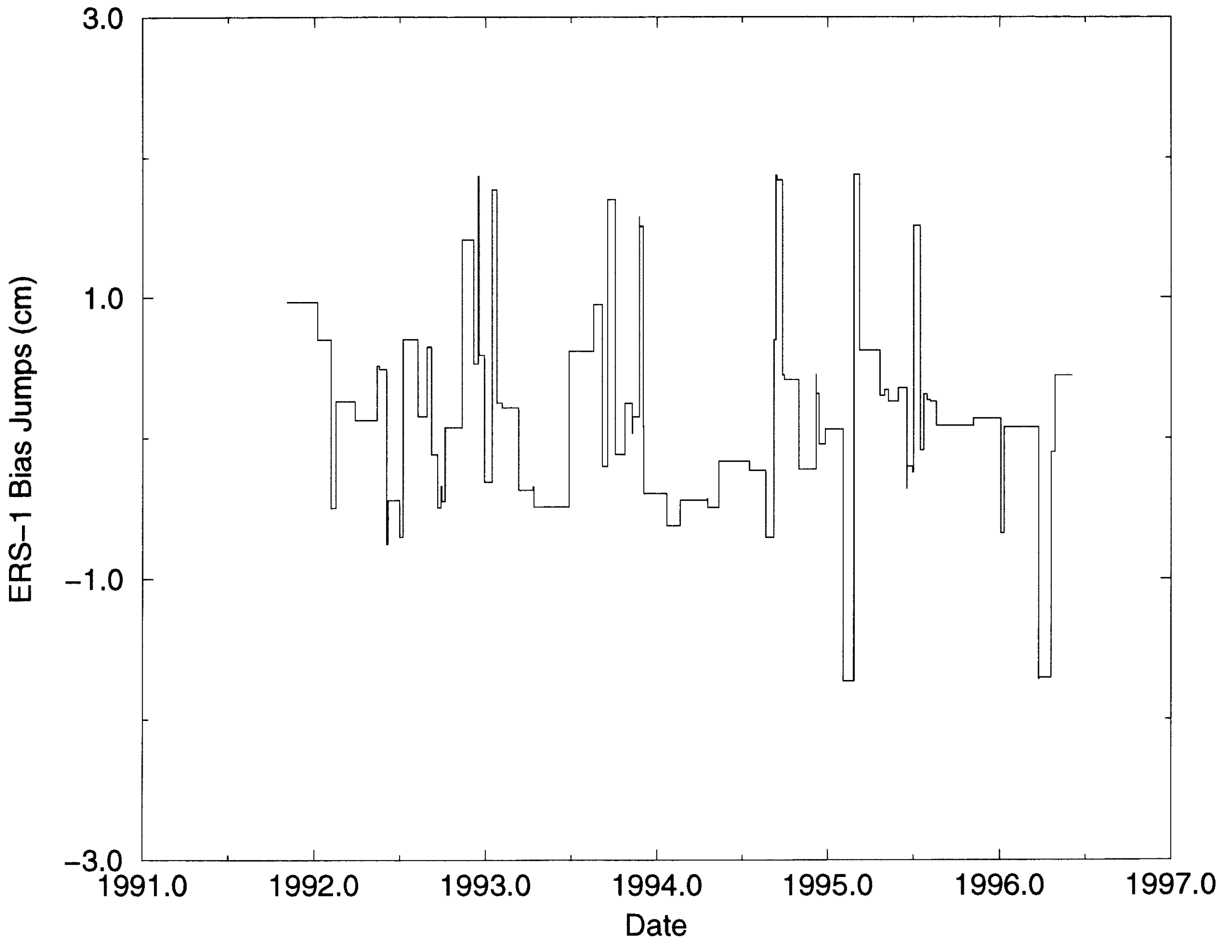

Figure 4. ERS-2 Ultra Stable Oscillator (USO) corrections (as supplied by ESRIN)

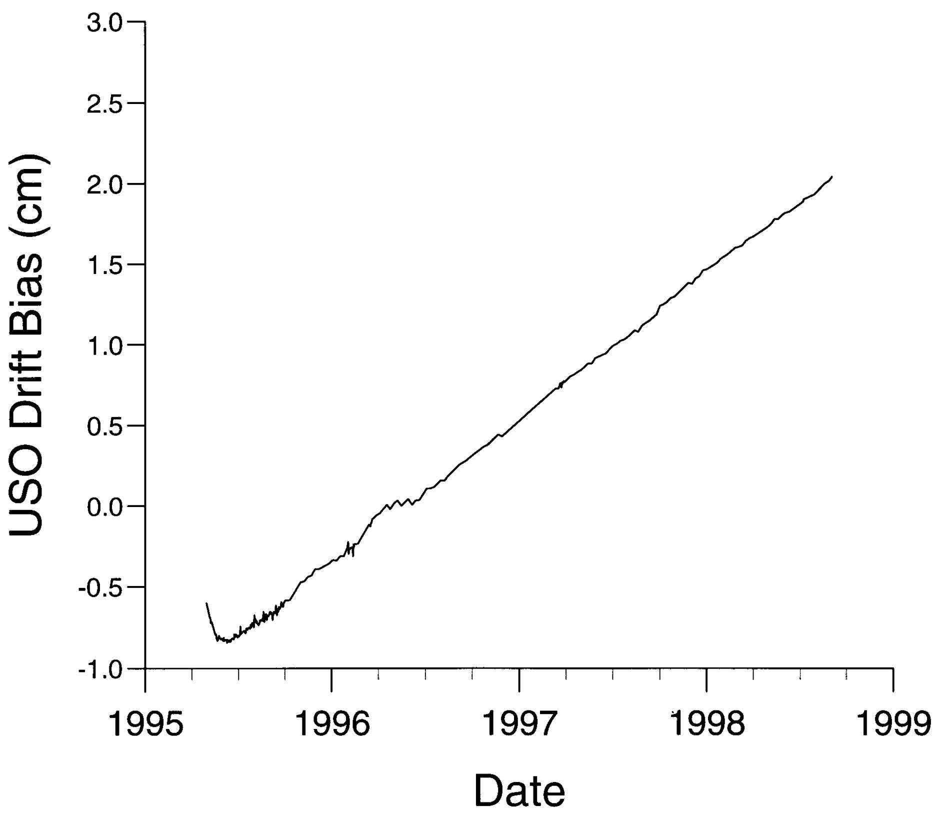

Figure 5. ERS−2 bias jumps as characterised by SPTR

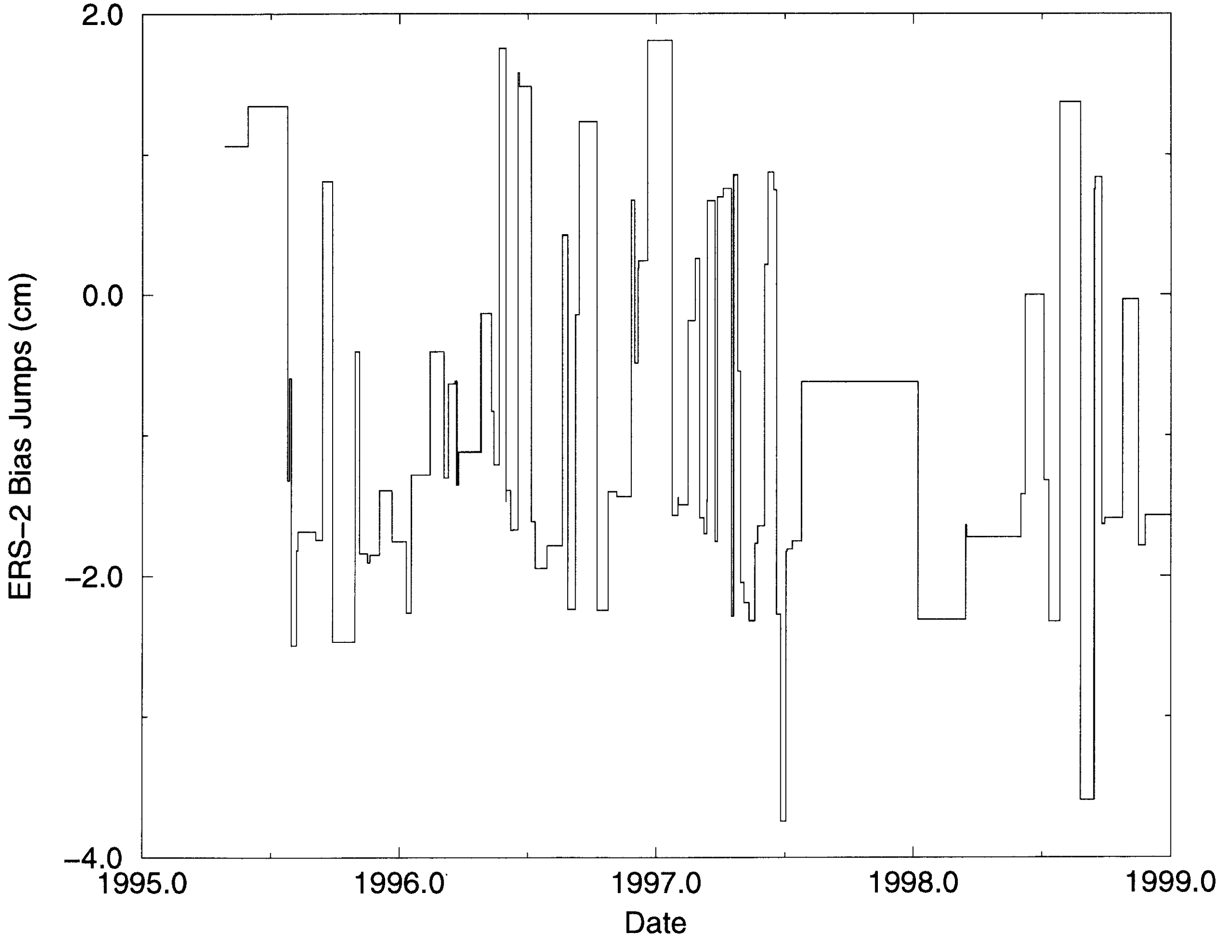

4. ERS orbits

Orbital heights for ERS are available from various sources including the DPAF orbit on the CD ROM, Delft University (DUT) and the Center of Space Research, Texas. However as we needed to compute dual crossovers it was decided to utilise ERS orbits computed in-house using the *FAUST* software suite (Boomkamp, 1999). For ERS-1 laser range data and single satellite crossovers (SXO) for epochs differing by 5 days or less were used as tracking data. For ERS-2 the tracking was augmented by PRARE data. *FAUST* has a multi-arc capability enabling an individual arc of typically 5 days in length to be connected to the following arc through the SXO data; thus reducing the discontinuity in radial orbital height between the two arcs. In practice, there is no restriction on the number of arcs that can be adjoined in this manner but, for computation ease, total arc lengths were restricted to about 45 days; namely a complete repeat cycle of 35 days and an overlap arc at the start and end of the multi-arc period.

Gravity field modelling is crucial to orbital accuracy. JGM-3 (Tapley et al, 1996) was derived with TOPEX/Poseidon in mind with estimated radial precision of near 3 cm (Marshall et al, 1995) and SXO residuals very close to 7.0 cm rms (AVISO, 1998) For ERS the DPAF orbits employ PGM035 or PGM055 with SXO residuals about 11-12 cm at best. Several groups have undertaken gravity field refinements to produce a model tailored to the specific orbital characteristics of ERS. In particular, DEOS, Delft University of Technology have produced an enhanced gravity field DGM-E04 and associated orbits for the ERS-1 and ERS-2 missions (Scharroo and Visser, 1998). DEOS refined a subset of the JGM-3 coefficients by minimising ERS-1 SXO residuals.

Mathematically the radial error, Δr, due to gravitational mismodellng (Rosborough, 1986) can be written as

$$\Delta r = \Delta f + \delta_{A/D}\,\Delta v$$

where Δf is the geographically correlated error which is invariant for a particular satellite orbit at a given geographical location; Δv the so-called anti-correlated term and $\delta_{A/D}=\pm 1$, with sign changing from an ascending pass (A) to a descending pass (D). Thus at a SXO location the error in Δ_{SXO} (Equation 5) is $\pm 2\Delta v$. SXO residuals provide a measure of the geographically anti correlated term but the geographically correlated component, Δf, is unobservable.

The DEOS methodology has the advantage of tuning the geopotential coefficients to minimise the gravity field error observable in SXO data, i.e Δv, and by inference reducing the geographically correlated gravity field component, Δf. In contrast to this approach, Aston produced AGM98 through a fully dynamic procedure by minimising tracking residuals from both ERS-1 and TOPEX/Poseidon over the period of the second 168 days of the ERS-1 geodetic mission. For AGM98, tracking data included laser ranging and SXO data for ERS-1; laser range and DORIS tracking for

TOPEX/Poseidon and dual crossover (DXO) data to link the two orbits. DXO data provides a measure of both the anti correlated error, Δv, and the geographically correlated term, Δf.

A comparison of the resultant ERS-1 geographically correlated and anti correlated errors within the DUT DGM-E04 and Aston AGM98 orbits has been performed at Aston as part of research external to this study. DXO residuals between ERS-1 and TOPEX/Poseidon for epochs differing by 5 days or less were collated for the various ERS-1 orbital phases. By assuming that the TOPEX/Poseidon error is small, the mean error for ascending and descending ERS-1 passes can be extracted for say 2° lat. by 4° long. bins. Simple addition (subtraction) then yields twice the geographically correlated (anti correlated) errors for the gravity field model. Figure 6 presents typical plots of these errors for JGM-3, DGM-E04 and AGM98 for the second ERS-1 multidisciplinary phase. This phase has the same orbital characteristics as that of ERS-2. Note the difference in scale for JGM-3. The Figure shows that both DGM-E04 and AGM98 are significant enhancements over JGM-3. We note that DGM-E04 performs best for the anti correlated error with AGM98 best for the geographically correlated errors. In reality, these inferences merely reflect the underlying data sets used in construction of the enhancements. The overall rms. radial errors of gravitational origin for the second ERS-1 multidisciplinary phase are 4.86 cm for JGM-3, 2.64 cm for DGM-E04 and 2.44 cm for AGM98. There is thus little to choose between DGM-E04 and AGM-98 although, given the use of DXO and repeat pass data herein for ERS and TOPEX/Poseidon inter-calibrations, it makes sense to use AGM98 where the orbital errors are spread more equally across the geographically correlated and anti correlated components. A similar study has been performed for the DPAF orbits with the observation that these are inferior to both DUT and Aston orbits. This is not a reflection on the DPAF capability but rather a consequence of the requirement that orbital modelling remains relatively consistent over the CD ROM orbits. Other groups can enhance ERS positioning with ease and release orbits over the Internet as orbital strategies change. DPAF does not have this flexibility. Hereafter, only AGM98 will be used.

Aston AGM98 orbits for ERS-1 and ERS-2 were produced using

- SLR, single satellite crossovers, PRARE
- AGM98 gravity field
- DTM94 thermospheric model
- ITRF96 SLR station coordinates
- Aston station coordinates for PRARE.
- Multi-arcs of typically 45 day duration comprising say nine five day arcs

The solution set included

- initial position and velocity for each arc
- 6 hr drag scale factors
- daily 1 cy/rev along track and cross track empirical accelerations
- time tag bias for ERS-2 altimetry
- PRARE range bias per station per multi-arc.

- PRARE tropospheric correction scaling factor per pass

Each multi-arc solution comprised typically nine 5 day arcs giving an arc overlap at the start and end of each solution from which the central 35 days were utilised. In terms of the quantity of tracking data (see Table 1) we observe that SLR data tends to decrease in the winter months in the Northern Hemisphere - as expected from the predominance of stations in Europe and the USA - and that the overall numbers have increased as more stations become reliable and hence contribute profitably to orbital work. The quantity of SXO data shows the expected trends with maximum in the Southern Hemisphere summer due to the retreat of sea ice. The PRARE tracking system was introduced for ERS-1 but, as is well known, failed soon after launch. After testing on a Russian Meteor satellite the space segment on ERS-2 was validated in late 1995. The number of ground stations was gradually increased to the extent that, by mid 1996, the numbers of range and range rate measurements numbered over 40000 per 45 day period. After peaking close to 70000 range measurements the numbers began to decrease as some stations became inoperational and dropped out of the network.

A summary of the orbital computations are presented in Table 1. The SLR residuals are typically 4-7cm, SXO residuals 7-8 cm, PRARE range measurements 6-7 cm and PRARE range rate residuals 0.06-0.07 mm/sec. Given that range residuals are usually dominated by the along-track error and that SXO residuals includes a large error component from the altimetric corrections etc we can infer that the radial error is probably at the 5cm level or better for most arcs. The 7-8 cm SXO rms residual is not far short of the 7.0 cm value quoted for TOPEX/Poseidon.

cy	yr	mth	day	-yr	mth	day	MJD1	MJD2	#SLR	rms	#SXO	rms	#P ra	rms	#P rr	rms
1	95	5	16	95	6	25	49853	49893	5228	3.72	7235	7.48				
2	95	6	15	95	7	30	49883	49928	5503	4.02	8342	7.11	321	6.20	328	0.54
3	95	7	20	95	9	2	49918	49962	8799	5.16	7579	7.18	1405	6.87	1472	0.64
4	95	8	24	95	10	7	49953	49997	7541	4.84	6200	7.32	3658	7.33	3385	0.58
5	95	9	27	95	11	10	49987	50031	8712	5.32	7473	7.55	8463	6.81	8079	0.59
6	95	11	1	95	12	18	50022	50069	5430	4.26	8068	7.73	9163	7.37	9399	0.65
7	95	12	8	96	1	22	50059	50104	5041	5.52	8186	7.74	20219	7.37	21318	0.66
8	96	1	11	96	2	27	50093	50140	6630	5.87	8780	7.69	23239	7.03	23639	0.62
9	96	2	17	96	3	29	50130	50171	7972	6.27	8791	7.26	31321	7.66	30893	0.70
10	96	3	23	96	5	5	50165	50209	9991	6.17	9062	7.55	28321	7.31	30951	0.67
11	96	4	26	96	6	7	50199	50241	8372	5.62	6997	7.38	26583	7.47	27331	0.76
12	96	5	30	96	7	16	50233	50280	9372	5.60	8522	7.43	34486	6.86	38704	0.70
13	96	7	2	96	8	21	50266	50316	11371	6.93	8748	7.81	47589	7.13	48411	0.69
14	96	8	10	96	9	22	50305	50348	8220	7.72	7032	7.41	41345	7.12	42387	0.72
15	96	9	12	96	10	29	50338	50385	8314	6.67	8833	7.46	51212	6.80	50534	0.69
16	96	10	19	96	12	3	50375	50420	5708	5.63	8073	7.55	46742	6.38	34405	0.63
17	96	11	23	97	1	7	50410	50455	4116	5.87	8767	7.69	51443	6.62	48902	0.61
18	96	12	25	97	2	10	50442	50489	5754	6.63	11364	7.55	64154	6.75	59648	0.63
19	97	1	28	97	3	16	50476	50523	8770	7.26	7709	8.30	62399	7.33	58573	0.69
20	97	3	8	97	4	22	50515	50560	10063	7.50	8861	9.07	62174	7.58	58060	0.72
21	97	4	10	97	5	25	50548	50593	8752	5.84	7325	7.47	60610	7.36	56479	0.69
22	97	5	5	97	7	1	50583	50630	8944	5.99	9017	7.38	72364	7.16	69991	0.63
23	97	6	19	97	8	5	50618	50665	9313	5.77	8479	7.37	73015	7.10	70215	0.63
24	97	7	24	97	9	7	50653	50698	10339	6.01	7912	7.50	62345	6.67	59578	0.59
25	97	8	28	97	10	12	50688	50733	10614	5.28	8127	7.44	53417	6.76	53673	0.63
26	97	10	2	97	11	16	50723	50768	6855	5.25	8829	7.92	44657	6.99	48539	0.68
27	97	11	4	97	12	21	50756	50803	6202	5.47	9388	7.59	50521	7.05	51440	0.71
28	97	12	10	98	1	25	50792	50838	5984	6.45	11534	8.43	51038	7.35	47757	0.66
29	98	1	20	98	3	1	50833	50873	8482	7.70	12413	8.21	52118	7.88	48270	0.69

30	98	2	24	98	4	5	50868	50908	7235	7.66	9177	8.08	43119	8.03	38514	0.73
31	98	3	26	98	5	10	50898	50943	7978	7.03	9000	8.66	46541	7.98	40670	0.76
32	98	5	2	98	6	14	50935	50978	7552	6.72	9707	8.27	32254	7.57	28796	0.75
33	98	6	9	98	7	14	50973	51008	4939	5.85	8146	7.71	20780	8.17	19324	0.70

Table 1. Tracking data residuals for cycles 1 - 33 of ERS-2. Column 1 gives the cycle no; columns 2-4 and 5-7 the date of the start and end day for each arc; columns 8 and 9 give the corresponding Modified Julian Date; the number of measurements and the rms. of fit are given in the remaining columns in the order SLR, SXO, PRARE range and PRARE range rate. All rms. values are in cm except the final column (PRARE range rate) which is mm/sec.

Figure 6a. JGM-3 geographically correlated and anti correlated gravitational errors for ERS-1 second multidisciplinary phase.

JGM-3 Anti Correlated Error (Multi 2)

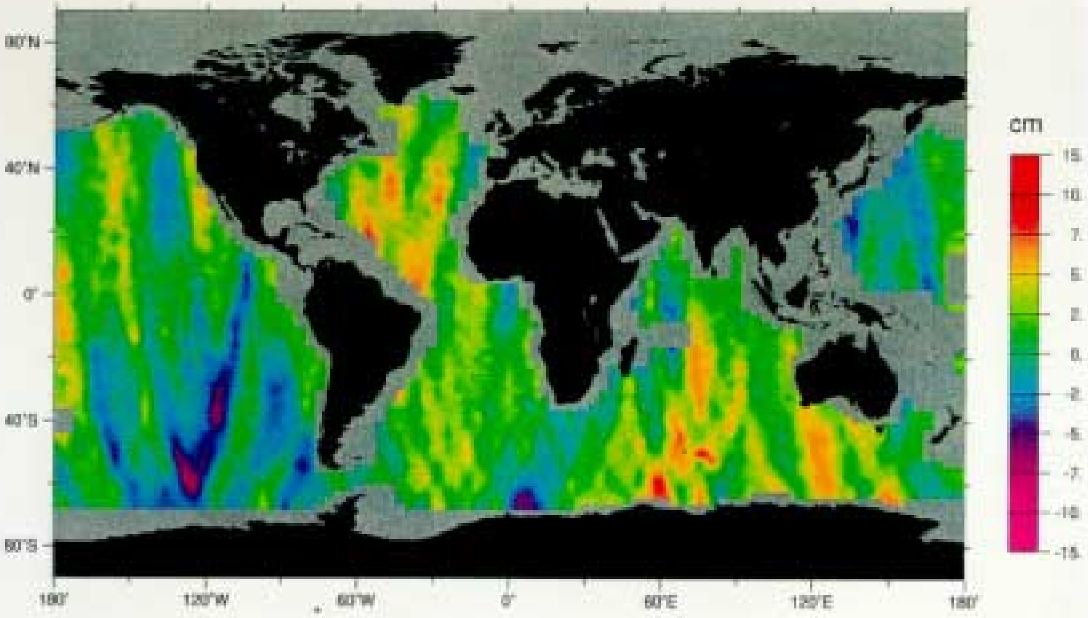

JGM-3 Correlated Error (Multi 2)

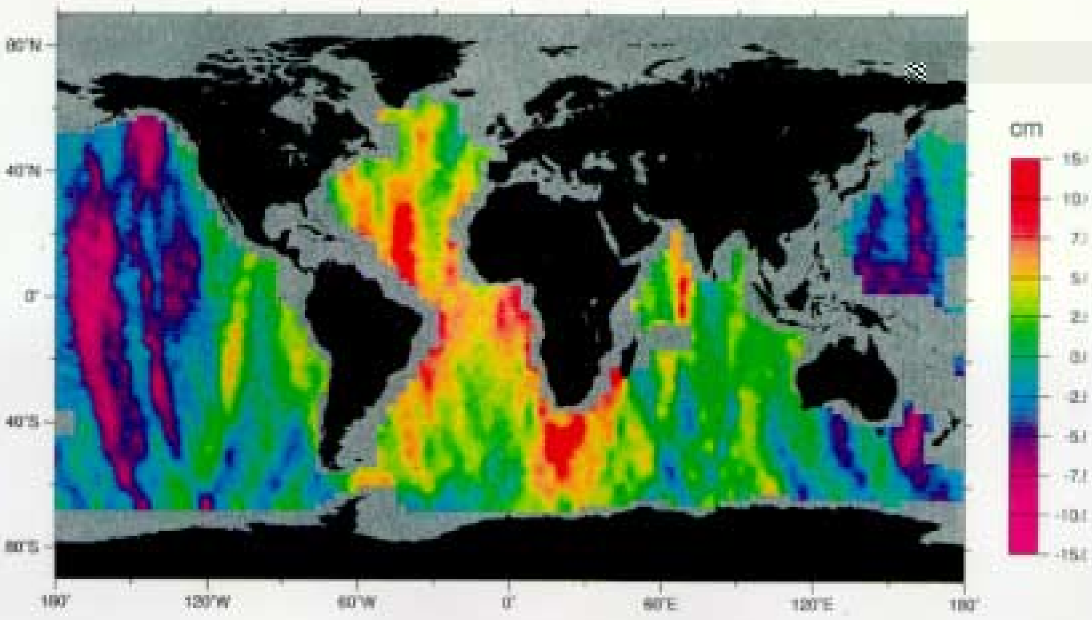

Figure 6b. DGM-E04 geographically correlated and anti correlated gravitational errors for ERS-1 second multidisciplinary phase.

DGM-4 Anti Correlated Error (Multi 2)

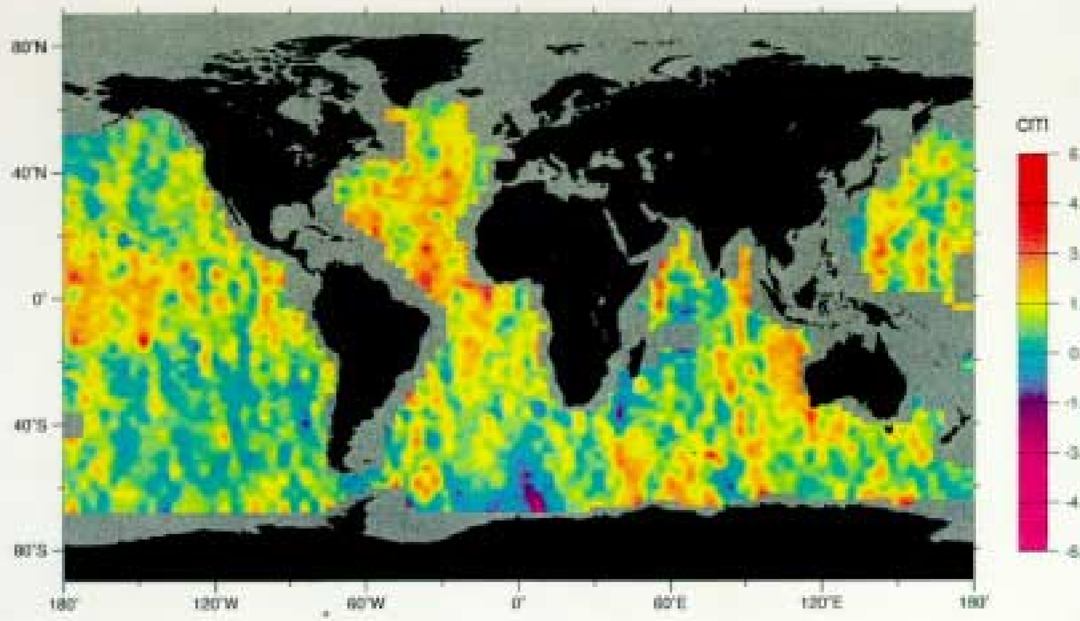

DGM-4 Correlated Error (Multi 2)

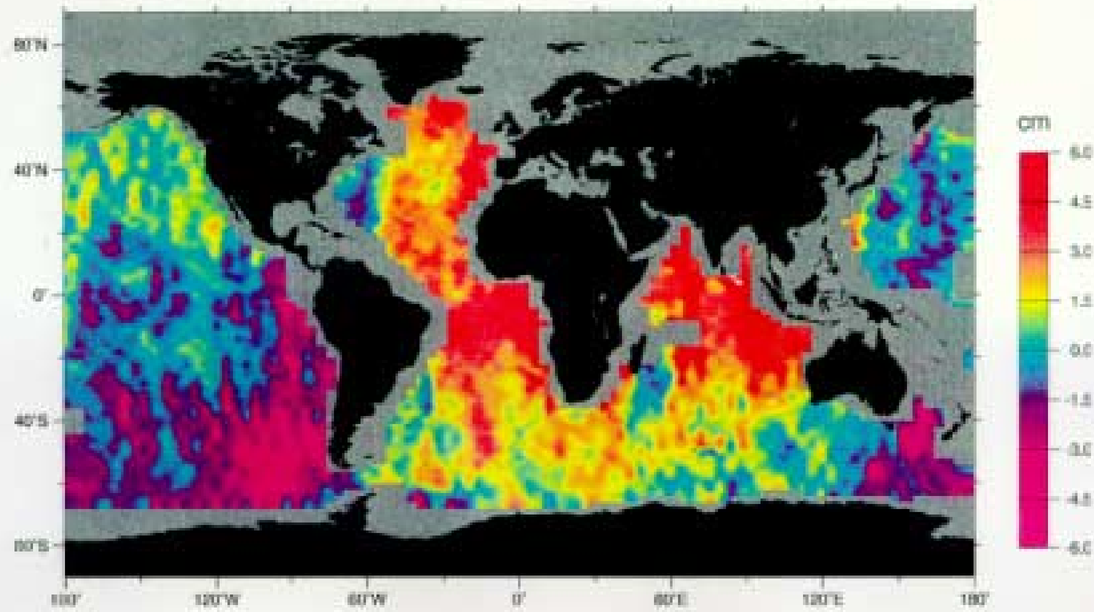

Figure 6c. AGM98 geographically correlated and anti correlated gravitational errors for ERS-1 second multidisciplinary phase.

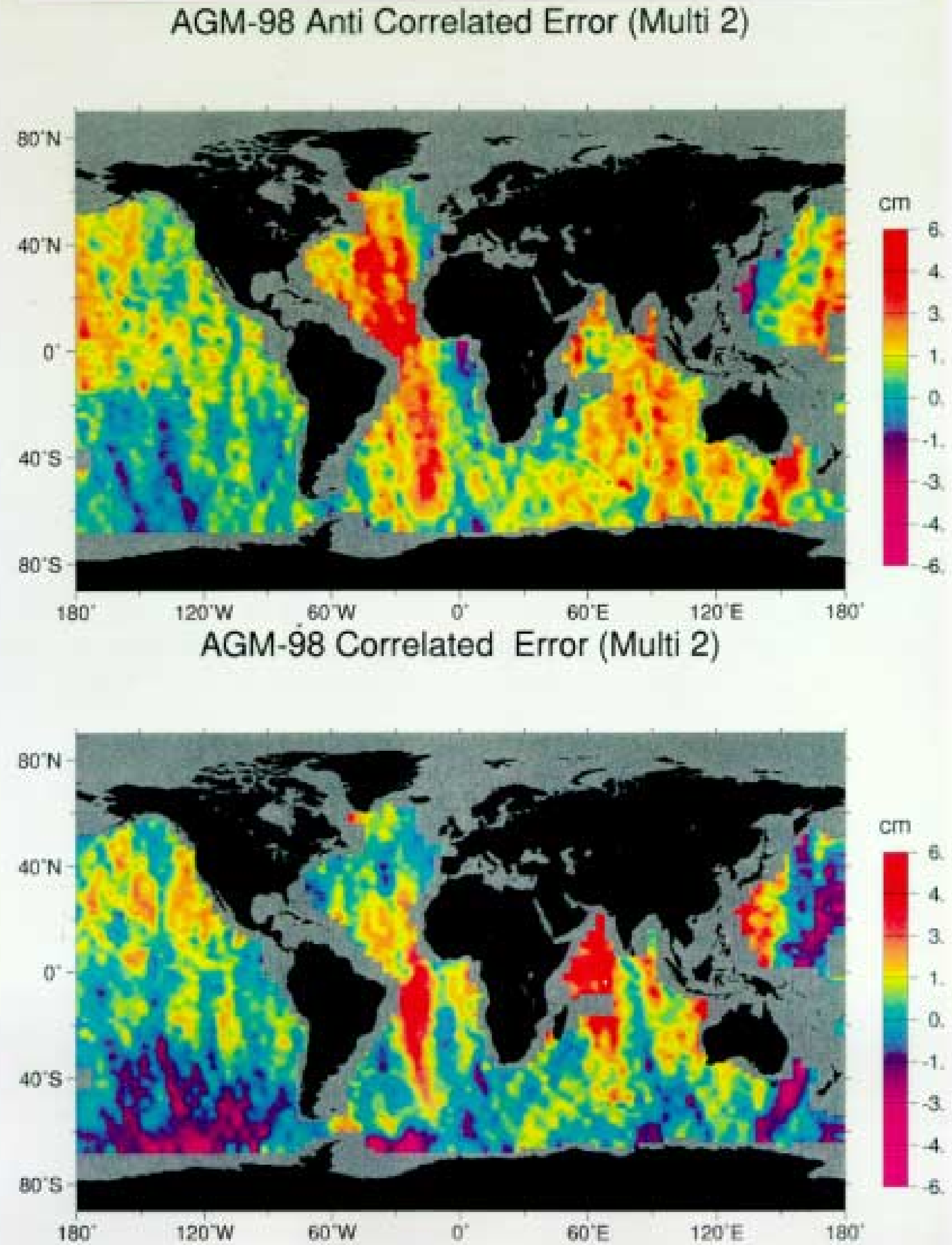

5. Tide gauge verification

In situ tide gauge data has been used previously for absolute and relative calibration of altimetric satellites. For absolute calibrations, such as the Venice Tower for ERS-1 (Francis, 1993) and Harvest Platform for TOPEX/Poseidon (Christensen et al, 1994), the tide gauge is tied geocentrically to the tracking network by precise GPS measurements. Although few tide gauges are collocated with GPS receivers that does not prevent the global network being employed to monitor the stability of the altimeter bias drift. Relative monitoring has been used to great effect to determine the drift in TOPEX (Nerem et al, 1997) and to examine the stability of ERS-1 (Moore et al, 1999). The procedure has certain requirements, foremost of which is to ensure that the tide gauge time series is representative of that observed by the altimeter and not corrupted by local effects. Further, as tide gauges are connected to land, any local land motion will be aliased into the tide gauge records. Fortunately most tide gauges are sited away from the centre of the last glaciation with post-glacial rebound being near negligible. However, local land motion is well known to be evident in several tide gauge time series and these must be eliminated in advance.

Tide gauge data is available for 109 gauges in the FASTWOCE data set with releases in daily or monthly tables. For this study the better temporal sampling of the daily records is required. Contrary to the name, tide gauge data does not record the short-term ocean tides as, in practice, these are removed by filtering 119 hourly values centred at the midday of the day in question. Tide gauges thus reflect variability in the ocean surface from currents, meteorological forcing etc. Tide gauges provide a simple mechanism for both monitoring and replicating the temporal signatures in the altimetry.

To examine the validity of each of the 109 gauges in the FASTWOCE release we employed TOPEX/Poseidon data. Repeat pass TOPEX (NRA) altimetry at the latitude of the tide gauge was extracted for the two ascending and two descending passes closest to the gauge for cycles 1-219, Sept 1992 to Sept 1998. This yielded a total of 330 repeat pass locations. Time series of ocean variability for each location was then compared directly against the tide gauge time series interpolated to the required epochs. A correlation analysis and linear regression of the differences supplied a measure of the reliability of a particular gauge. Repeat pass locations were deemed acceptable if

- the number of cycles contributing to the time series exceeded 140 out of a possible maximum of 198. Note that 21 of the total 219 cycles considered were entirely Poseidon.
- the correlation coefficient exceeded 0.3
- the rms. difference between altimetry and tide gauge time series was 10.0 cm or less.
- linear regression of the differences resulted in a slope of 15 mm/yr or less in absolute value.

204 of the original 330 repeat pass time series passed these acceptance criteria but 30 gauges were eliminated, leaving 79 for subsequent analysis.

The accepted tide gauges are summarised in Table 2. Table 3 further lists the tide gauge identification number, T/P arc number, rms. agreement and correlation between the tide gauge and altimetric time series, number of T/P cycles contributing to the altimetric time series and the slope of the linear regression analysis. The global distribution of the remaining 79 gauges is given as Figure 7 with their periods of operation shown in Figure 8.

Figure 7. WOCE tide gauge used in TOPEX analysis

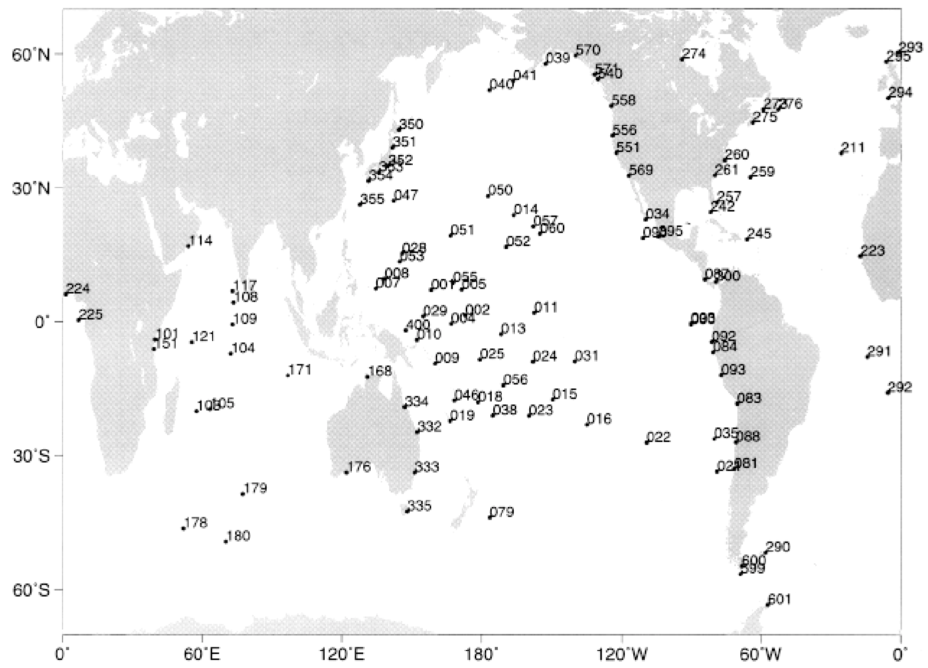

Figure 8. Periods of operation for the 79 tide gauges of the FASTWOCE data set used in the stability analyses.

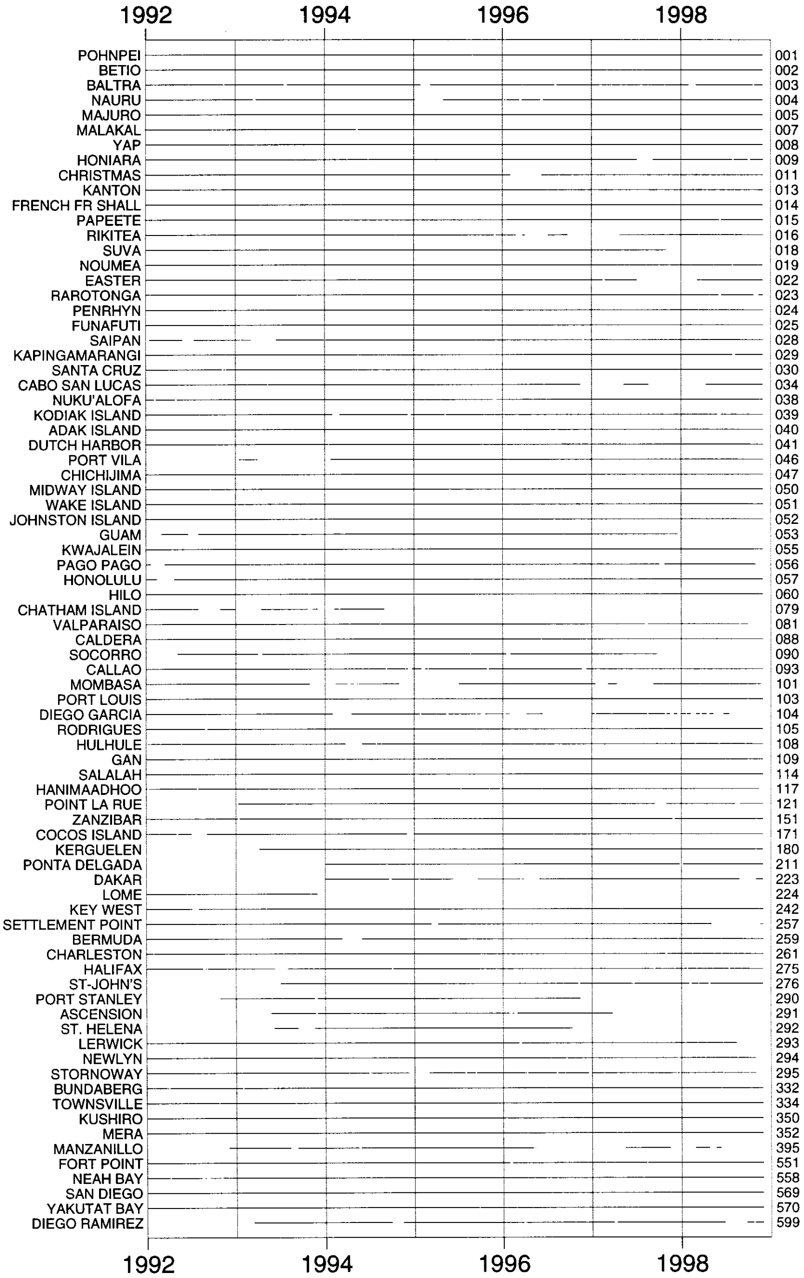

TG	Site	Lat	Long	
001	POHNPEI	06 59N	158 15E	Fd. St. Micronesia
002	BETIO	01 22N	172 56E	Kiribati
003	BALTRA	00 26S	090 17W	Galapagos Ecuador
004	NAURU	00 32S	166 54E	Nauru
005	MAJURO	07 06N	171 22E	Marshall Islands
007	MALAKAL	07 20N	134 28E	Belau
008	YAP	09 31N	138 08E	Fd. St. Micronesia
009	HONIARA	09 26S	159 57E	Solomon Islands
011	CHRISTMAS	01 59N	157 28W	Kiribati
013	KANTON	02 49S	171 43W	Kiribati
014	FRENCH FR SHALL	23 52N	166 17W	Hawaii U.S.A.
015	PAPEETE	17 32S	149 34W	French Polynesia
016	RIKITEA	23 08S	134 57W	French Polynesia
018	SUVA	18 08S	178 26E	Fiji
019	NOUMEA	22 18S	166 26E	New Caledonia
022	EASTER	27 09S	109 27W	Chile
023	RAROTONGA	21 12S	159 47W	Cook Islands
024	PENRHYN	08 59S	158 03W	Cook Islands
025	FUNAFUTI	08 32S	179 13E	Tuvalu
028	SAIPAN	15 14N	145 45E	Mariana Islands
029	KAPINGAMARANGI	01 06N	154 47E	Fd. St. Micronesia
030	SANTA CRUZ	00 45S	090 19W	Galapagos Ecuador
034	CABO SAN LUCAS	22 53N	109 55W	Mexico
038	NUKU'ALOFA	21 08S	175 10W	Tonga
039	KODIAK ISLAND	57 44N	152 31W	Alaska U.S.A.
040	ADAK ISLAND	51 52N	176 38W	Alaska U.S.A.
041	DUTCH HARBOR	53 54N	166 30W	Alaska U.S.A.
046	PORT VILA	17 46S	168 18E	Vanuatu
047	CHICHIJIMA	27 06N	142 11E	Japan
050	MIDWAY ISLAND	28 13N	177 22W	U.S.A. Trust
051	WAKE ISLAND	19 17N	166 37E	U.S.A. Trust
052	JOHNSTON ISLAND	16 45N	169 31W	U.S.A. Trust
053	GUAM	13 26N	144 39E	U.S.A. Trust
055	KWAJALEIN	08 44N	167 44E	Marshall island
056	PAGO PAGO	14 17S	170 41W	Samoa U.S.A
057	HONOLULU	21 18N	157 52W	Hawaii U.S.A
060	HILO	19 44N	155 04W	Hawaii U.S.A
079	CHATHAM ISLAND	43 57S	176 34W	New Zealand
081	VALPARAISO	33 02S	071 38W	Chile
088	CALDERA	27 04S	070 50W	Chile
090	SOCORRO	18 44N	111 01W	Mexico
093	CALLAO	12 03S	077 09W	Peru
101	MOMBASA	04 04S	039 39E	Kenya
103	PORT LOUIS	20 09S	057 30E	Mauritius
104	DIEGO GARCIA	07 17S	072 24E	United Kingdom
105	RODRIGUES	19 40S	063 25E	Mauritius
108	HULHULE	04 11N	073 32E	Republic of Maldives
109	GAN	00 41S	073 09E	Republic of Maldives
114	SALALAH	16 56N	054 00E	Oman
117	HANIMAADHOO	06 46N	073 10E	Maldives
121	POINT LA RUE	04 40S	055 32E	Seychelles
151	ZANZIBAR	06 09S	039 11E	Tanzania
171	COCOS ISLAND	12 07S	096 54E	Australia
180	KERGUELEN	49 21S	070 13E	France
211	PONTA DELGADA	37 44N	025 41W	Azores
223	DAKAR	14 40N	017 26W	Senegal
224	LOME	06 08N	001 17E	Togo
242	KEY WEST	24 33N	081 49W	Florida U.S.A.
257	SETTLEMENT POINT	26 43N	078 60W	Bahamas United Kingdom
259	BERMUDA	32 22N	064 42W	United Kingdom
261	CHARLESTON	32 47N	079 56W	South Carolina U.S.A.
275	HALIFAX	44 40N	063 35W	Canada
276	ST-JOHN'S	47 34N	052 43W	Canada
290	PORT STANLEY	51 45S	057 56W	United Kingdom
291	ASCENSION	07 55S	014 25W	United Kingdom

292	ST. HELENA	15 58S 005 42W	United Kingdom
293	LERWICK	60 09N 001 08W	United Kingdom
294	NEWLYN	50 06N 005 33W	United Kingdom
295	STORNOWAY	58 13N 006 23W	United kingdom
332	BUNDABERG	24 50S 152 21E	Australia
334	TOWNSVILLE	19 15S 146 50E	Australia
350	KUSHIRO	42 58N 144 23E	Japan
352	MERA	34 55N 139 50E	Japan
395	MANZANILLO	19 03N 104 20W	Mexico
551	FORT POINT	37 48N 122 28W	California U.S.A
558	NEAH BAY	48 22N 124 37W	Washington U.S.A.
569	SAN DIEGO	32 43N 117 10W	California U.S.A.
570	YAKUTAT BAY	59 33N 139 44W	Alaska U.S.A.
599	DIEGO RAMIREZ	56 31S 068 43W	Chile

Table 2. Tide gauge identification number and location for accepted sites.

TG ID	T/P pass	correlation	rms (cm)	# cycles	slope(mm/yr)
1	162	0.85	5.94	186	-7.0
1	175	0.88	5.45	179	-2.9
1	251	0.92	4.43	182	-2.6
2	34	0.92	3.88	180	-3.3
2	110	0.87	4.57	187	0.7
2	123	0.86	4.86	188	-2.4
2	199	0.84	5.13	187	-0.3
3	154	0.90	5.20	193	2.5
3	167	0.91	5.16	192	1.7
3	243	0.84	6.71	176	9.8
4	47	0.83	5.94	183	2.3
4	136	0.85	5.63	184	3.3
4	212	0.84	5.45	184	-0.9
4	225	0.84	5.61	176	-2.2
5	34	0.88	5.14	175	-1.7
5	47	0.92	4.32	180	1.3
5	110	0.91	4.66	181	-2.6
5	123	0.90	4.87	182	-3.6
7	62	0.82	6.97	182	-2.5
7	75	0.89	5.78	181	3.6
7	138	0.91	5.32	179	3.1
7	151	0.81	7.62	168	3.0
8	36	0.78	6.80	175	3.0
8	151	0.83	6.28	184	-0.7
8	214	0.88	5.16	183	-1.0
8	227	0.83	6.04	177	0.5
9	86	0.89	5.99	186	0.9
9	149	0.92	5.19	184	3.6
9	225	0.85	6.57	167	-7.9
11	32	0.87	5.32	188	-7.1
11	121	0.86	5.52	193	-5.2
13	71	0.87	3.77	186	-3.4
13	147	0.87	3.74	192	-3.4
13	160	0.85	4.12	191	-5.4
13	236	0.85	4.48	179	-1.2
14	108	0.79	6.35	194	-8.1
14	249	0.81	5.89	191	-7.7
15	69	0.76	4.01	189	2.4
15	108	0.69	4.61	191	4.0
15	145	0.60	5.01	184	-0.6
15	184	0.58	5.15	190	-1.9
16	17	0.75	4.86	183	-4.0
16	93	0.31	8.12	189	-7.4
16	158	0.54	7.12	182	-2.9
16	234	0.49	7.22	174	2.8
18	34	0.73	5.73	165	-9.2
18	71	0.59	6.70	184	-11.9
18	212	0.68	5.86	188	1.3
19	21	0.50	8.90	186	4.5
19	86	0.45	9.12	192	4.0
19	199	0.65	6.17	191	4.4
22	4	0.52	6.90	187	5.2
22	15	0.58	9.58	183	-4.4
22	80	0.79	4.64	185	-1.1
22	193	0.52	6.71	187	6.4
23	58	0.67	8.74	160	7.3
23	95	0.61	7.64	192	7.6
23	171	0.33	9.82	187	9.6
24	19	0.76	4.65	186	0.2
24	32	0.73	5.11	176	0.3
24	95	0.60	5.82	186	-3.6
24	210	0.71	5.44	185	-6.5
25	110	0.94	3.92	189	-0.6
25	186	0.92	4.52	185	-5.0

25	249	0.86	5.98	175	-4.5
28	49	0.84	5.42	188	6.5
28	125	0.60	8.67	194	9.8
28	188	0.80	6.09	190	4.9
29	10	0.82	6.65	175	6.6
29	175	0.84	6.08	183	5.7
29	251	0.89	5.14	180	3.0
30	154	0.93	4.15	191	0.1
30	167	0.91	5.21	192	-3.3
30	243	0.76	8.23	170	-0.3
34	104	0.61	9.12	191	-6.5
38	110	0.63	7.40	188	-5.8
38	147	0.66	7.02	189	-4.1
38	223	0.60	8.53	178	-13.1
39	54	0.89	7.08	186	5.3
39	123	0.89	6.83	190	7.8
40	99	0.85	7.46	182	6.0
41	132	0.84	8.47	186	12.2
46	21	0.63	7.76	173	12.2
46	60	0.54	8.05	180	13.7
46	199	0.57	7.37	180	3.1
46	238	0.67	7.42	173	9.8
47	10	0.85	7.97	178	6.4
50	58	0.46	9.78	187	0.3
50	123	0.77	6.10	192	-1.9
50	134	0.67	7.32	188	2.2
51	110	0.60	8.93	192	-6.9
52	134	0.47	9.19	194	3.1
52	210	0.74	7.34	193	3.0
52	249	0.83	5.68	191	3.1
53	10	0.72	8.83	180	5.9
53	49	0.80	7.77	183	2.3
53	125	0.73	8.76	185	10.2
55	34	0.82	4.75	180	-1.5
55	149	0.86	4.99	181	-3.2
55	212	0.86	4.73	192	-3.0
55	225	0.87	4.27	179	0.1
56	45	0.76	7.10	176	-9.4
56	84	0.90	4.40	189	-2.7
56	160	0.84	5.43	184	-2.6
56	223	0.83	5.94	171	2.4
57	6	0.64	6.06	184	4.0
57	45	0.45	7.57	189	1.2
57	82	0.54	6.82	195	-4.2
57	223	0.70	6.63	183	6.6
60	121	0.54	6.52	194	-5.8
60	158	0.52	7.12	192	-3.8
79	60	0.47	9.65	185	2.4
81	63	0.44	7.44	196	-5.1
81	230	0.47	9.89	185	0.5
88	52	0.44	7.22	195	4.4
88	241	0.41	7.19	185	-2.2
90	67	0.34	9.91	185	-9.3
93	52	0.67	7.53	196	1.1
93	191	0.75	7.02	198	7.4
101	5	0.51	9.32	188	5.5
101	18	0.56	6.09	186	2.3
103	29	0.60	8.78	183	0.3
103	105	0.81	5.57	191	-3.3
103	246	0.55	8.67	188	3.0
104	16	0.83	5.32	181	-2.8
104	79	0.80	5.79	182	-6.8
104	92	0.83	5.68	188	-6.2
104	155	0.75	7.08	181	-6.3
105	3	0.84	5.85	188	0.9
105	42	0.47	9.89	188	0.7

105	181	0.65	8.80	190	7.3
108	3	0.61	6.54	179	1.3
108	79	0.67	5.57	192	-1.3
108	168	0.80	4.27	190	-2.2
108	244	0.68	4.96	176	-4.6
109	3	0.64	5.19	181	-9.6
109	79	0.69	4.70	183	-10.4
109	92	0.65	5.26	188	-8.6
114	157	0.69	6.70	192	-0.9
117	3	0.82	6.44	185	-5.3
117	168	0.67	6.54	187	-6.2
117	181	0.70	5.88	192	-2.1
117	244	0.74	6.39	178	-11.5
121	55	0.83	6.19	175	-9.6
121	131	0.84	6.39	177	-6.5
121	144	0.87	5.54	176	-11.9
121	220	0.82	6.45	173	-5.5
151	5	0.49	7.39	188	10.8
151	18	0.46	7.26	187	9.8
171	1	0.78	7.80	181	5.3
171	77	0.75	7.94	190	1.0
171	116	0.72	8.68	186	3.4
171	192	0.86	5.89	189	1.0
180	103	0.77	7.81	168	14.1
211	11	0.76	6.57	143	-9.0
211	72	0.78	6.67	150	-0.6
211	189	0.74	7.03	144	8.5
211	250	0.83	5.02	140	-2.8
223	98	0.45	7.48	152	-4.5
223	213	0.50	7.46	151	8.9
224	122	0.35	9.09	172	-2.0
224	135	0.36	6.83	193	-0.5
242	102	0.72	8.98	150	2.0
242	167	0.68	7.57	187	7.3
242	243	0.75	8.20	179	8.1
257	65	0.58	9.40	195	-3.8
257	178	0.81	5.27	185	-1.0
257	243	0.81	5.60	182	-0.5
257	254	0.61	9.21	158	-8.7
259	39	0.80	9.15	183	5.7
259	126	0.75	9.49	188	7.4
261	167	0.90	6.47	183	-3.6
275	141	0.69	9.57	179	-11.4
276	48	0.79	8.57	140	-10.0
276	115	0.76	8.89	148	-12.2
290	137	0.63	9.31	188	-13.5
290	230	0.60	9.69	184	-9.8
291	9	0.50	3.67	172	-4.2
291	22	0.69	3.03	173	-5.5
291	85	0.47	4.37	173	-10.9
291	98	0.51	3.92	173	-5.1
292	59	0.50	4.63	172	10.2
292	135	0.61	3.91	171	3.4
292	174	0.56	4.00	172	7.2
292	250	0.54	4.32	170	0.4
293	94	0.93	6.66	190	-4.1
293	113	0.93	6.72	187	-1.0
293	170	0.87	7.79	190	-4.2
293	189	0.83	7.83	189	-6.7
294	248	0.78	8.25	184	-4.9
295	113	0.89	8.10	180	-3.7
332	36	0.60	8.57	188	-1.8
334	251	0.54	9.81	175	-3.3
350	136	0.60	9.02	168	-13.6
350	177	0.47	9.34	184	-4.2
352	177	0.61	9.73	174	-0.5

395	104	0.63	9.78	186	6.7
551	145	0.49	9.59	190	-11.5
558	104	0.88	7.74	170	0.9
569	119	0.69	6.08	194	-5.9
569	206	0.70	6.65	195	-3.8
570	21	0.90	7.80	176	9.6
599	61	0.80	8.76	173	4.3
599	206	0.81	9.70	170	6.8

Table 3. Summary of accepted T/P passes.

6. Stability of the TOPEX (NRA) altimetric range

The validation procedure of section 5 identified 204 repeat pass locations at 79 tide gauges for which the tide gauge time series can be used to adjust the altimetric series for ocean variability. The derived data set of tide gauge enhanced altimetric measurements can now be used for monitoring stability of the NRA altimetric measurement.

To combine all locations into a single data set the mean sea-level height at each location was derived as the mean of the second and third quartiles. This process eliminated the higher and lower quartiles but still left at least 70 measurements for establishing the mean offset. Once corrected for the appropriate mean sea-level height the residuals were analysed for the TOPEX altimetric bias.

The TOPEX bias was sought by two methods:-

- A step function with values constant over each TOPEX cycle. A single value was recovered from the 170-190 tide gauge enhanced altimetric measurements per cycle.
- A Gaussian weighting with decorrelation length near 16.5 days.

The TOPEX NRA bias drift along with their error bars are plotted as Figures 9 and 10 for these two methods. Figure 10 is by construction a smoothed version of Figure 9, the 16.5 day decorrelation time chosen to eliminate erratic change but to preserve the principle signals. Both Figures show a general linear decrease from launch until mid 1997 followed by a reversal in the trend. The early linear decrease is at least partly attributable to the corresponding drift in the TMR however the increase in 1997/8 requires a different explanation and may be an artefact of the deterioration of side A of the NRA altimeter onboard TOPEX/Poseidon. A drift in the side A measurements has been identified due possibly to a slow erosion of the point target response of the altimeter affecting both the range and significant wave height measurements. The net effect on the range is 1-2 cm. which is close to the observed upturn in Figure 9. A switch to side B was authorised in February 1999 in response to the hardware problems. Figures 9 and 10 show that the formal errors for the NRA drift are small; i.e. 4 mm for the step function in Figure 9 and 2 mm for the smoother Gaussian weighting of Figure 10. The importance of Figures 9 and 10 for ERS dual crossover inter-calibrations cannot be over emphasised as it is clearly incorrect to assume that the NRA is bias free with all signal attributable to ERS. For later application to ERS we prefer Figure 10 due to the inherent smoothing and the need to extract TOPEX bias drift values at the ERS epochs. Figure 10 also shows a clear annual signal with minimum in September/October. At the time of writing, we are uncertain whether the annual trend is a real signal in TOPEX or some spurious signal from the tide gauges.

Figure 9. TOPEX (NRA) bias drift determined as a step function constant over each cycle.

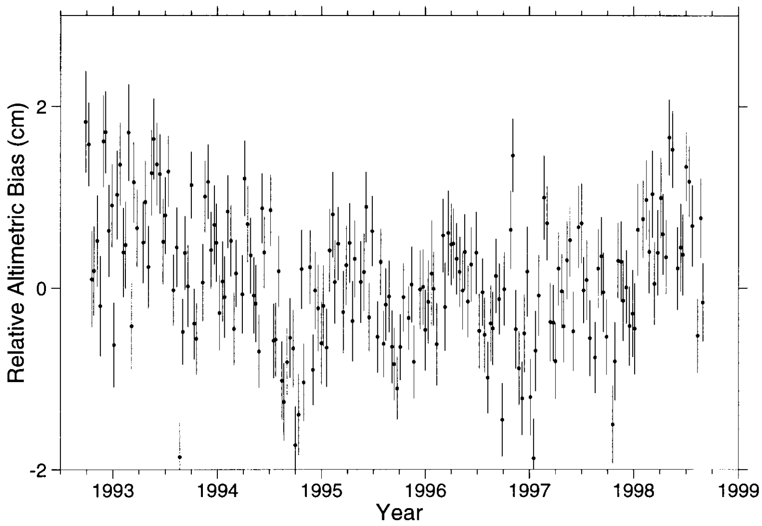

Figure 10. TOPEX (NRA) bias drift determined by Gaussian weighting with decorrelation length 16.5 days.

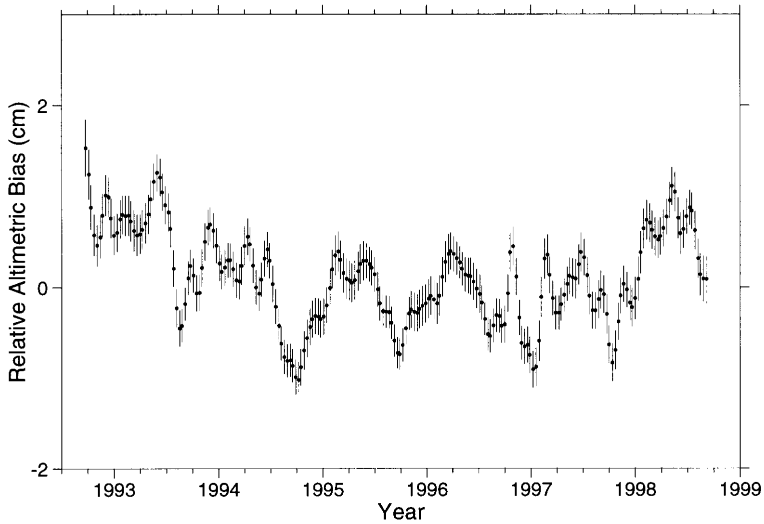

7. ERS bias drift: DXO results.

Dual crossover residuals between the two ERS satellites and TOPEX/Poseidon have been derived for epochs differing by 5 days or less. The choice of 5 days is somewhat arbitrary but is a compromise between larger time interval required for a good geographical distribution of the DXO locations and the smaller time interval required to mitigate against sea-surface change over the period. Whatever the chosen time period, DXO data set, and for the same reason SXO data, is dominated by high latitude data due to the curvature of the ground tracks. This dominance is amplified for TOPEX/Poseidon given the turning points in the ground track directions at the latitude extremes of 66.1°. In terms of the DXO data available, the domination by locations at higher latitudes means that the numbers available are influenced by the seasonal distribution of sea-ice in the Southern Oceans. Thus we note larger numbers of DXO data during the southern hemisphere summer than the icebound winter.

Dual crossover residuals for ERS-1 were derived from cycle 1 of TOPEX/Poseidon in October 1992 through cycle 137 corresponding to the ERS-1 deactivation in June 1996. The period encompassed ERS-1 cycles 5-18 of the Ist multidisciplinary phase C, the second ice phase D, the geodetic phases E and F and the 12 cycles of the 2nd multidisciplinary phase G. In total the data set comprised of 1339010 DXO residuals. As stated in section 3, the phase G data is version 6 which is incompatible with the earlier versions 3 - 5. In contrast the 1062575 DXOs between ERS-2 and TOPEX/Poseidon for the first 33 cycles of ERS-2 data from May 1995 - July 1998 are all version 6.

In addition to temporal variations in the altimeter bias the data will exhibit other possible trends, Δ^{dxo} (Equation 4), in the computation of the TOPEX/Poseidon and ERS DXO residuals. It has already been established that TOPEX exhibits certain signatures but for various reasons explained below we expect ERS to dominate the error budget for Δ^{dxo}. Firstly, despite the efforts in orbit determination and gravity field modelling, ERS positioning will always be less accurate than TOPEX/Poseidon. This is due primarily to the relative heights of 780 km and 1336 km and the associated attenuation of the gravity field with height. Air drag is also far more problematic at 780 km than at the altitude of TOPEX/Poseidon. Orbit error is also dependent to some extent on the tracking data available and despite the use of laser ranging (SLR), SXO data and PRARE (ERS-2), ERS is less well tracked than TOPEX/Poseidon with SLR and the truly global microwave system DORIS. An important consequence of dependence on SLR is its seasonal dependence due to inclement weather and cloud cover. A consequence of this is that the altimetric centre of figure for ERS and TOPEX altimetry may exhibit a seasonal signature as it is highly dependent on the geographical distribution of the tracking data used within the orbit determination. In terms of geophysical corrections, TOPEX benefits from being a dual frequency instrument enabling the ionospheric correction to be inferred from the time delays of the two frequencies rather than resorting to some model. The predominance of high latitude data also emphasises the importance of the sea-state bias models given the high wave heights and wind speeds in the Southern Ocean. With all empirical sea-state bias models inferred globally from single satellite crossover data and given a zonal distribution for wind speed and wave heights it is not inconceivable that the models favour the dominant regimes with a possible zonal signature to the error. Finally, TOPEX/Poseidon benefits from consistency of data processing with all cycles released as version C.

In view of the above comments it was considered advisable to solve for additional correction terms in the DXO residuals over each interval spanned by a constant relative bias. The correction terms involved included a relative bias between ERS and TOPEX (NRA) and/or Poseidon (SSALT); first order spherical harmonics to absorb any long-term temporal variation in the centre of figure; a timing bias for ERS altimetry and an empirical second order zonal term (with zero mean). The dual crossover residuals were thus fitted by

$$\Delta_{DXO} = A_{T/P}+A_3\cos\phi \cos\lambda + A_4\cos\phi \sin\lambda + A_5\sin\phi + A_6 r_\tau + A_7(\cos^2\phi - 0.5) \qquad (6)$$

where ϕ is the latitude; λ longitude; A_T, A_P the relative bias between ERS and TOPEX and Poseidon respectively; A_3 - A_5 coefficients of the 1st order spherical harmonics; A_6 the timing error; r_τ a function (Wagner and Klokocnik, 1994) of the Keplerian elements and A_7 the coefficient of the second order zonal term. In more detail the radial error r_τ due to a timing error $A_6=\tau$ is given by

$$r_\tau = n\, R_E \sin^2 I\, \{f + C_2\, (R_E / a)/2\}\, \sin 2u$$

where R_E is the mean equatorial radius (6378.1363 km); f the Earth's flattening (1/298.257), C_2 the Earth's unnormalised second zonal geopotential harmonic coefficient (-1082.63×10^{-6}); a, I, n the orbital semi-major axis, inclination and mean motion respectively and u the orbital argument of latitude.

The coefficients of equation (6) have been solved for each time interval between SPTR events. This lead to intervals as low as a single day and as high as 165 days. A rejection criterion of 25 cm was taken to remove spurious data after correction for the offset between TOPEX and ERS data of 43cm. Plots of the DXO derived coefficients and the error bars are plotted in Figure 11 for ERS-1 with the corresponding results for ERS-2 in Figure 12. In Figure 11 the various phases of the ERS-1 mission are separated by vertical lines. Both Figures reveal signatures in the relative bias. In particular there is a discontinuity at the beginning of the second multidisciplinary phase for ERS-1 delineating the introduction of version 6 data. The relative bias will be discussed in more detail below.

The importance of Figures 11 and 12 for bias studies is not the actual values of the coefficients per se but their long-term variation. A long-term temporal signal represents some, possibly unseen, change that may affect the bias drift stability if not accounted for. On considering the coefficients of Equation 6 it is possible to detect evidence of annual trends especially in A_3 for ERS-1. All coefficients A_3 - A_5 for ERS-1 have a negative mean indicating that the centre of figure of TOPEX/Poseidon and ERS-1 are offset probably due to small differences between the centre of figures of the tracking networks. A_6 for ERS-1 gave a mean near 1.6 ms which, in the more usual definition for the time tag bias as a correction to the altimetric observation time, indicates a time tag bias of -1.6 ms. Of more interest is the second order zonal harmonic coefficient A_7 which may give evidence of some discrepancy between high and equatorial latitudes. In Figure 11, A_7 oscillates around zero for the Ist multidisciplinary phase and 2nd ice phase but is negative for the geodetic and 2nd multidisciplinary phases. There appears to be no obvious explanation for this except that the OPR processing version changed to version 3.5 after the 2nd ice phase.

The results for ERS-2 can now be considered along side those of ERS-1. The corresponding time tag bias for ERS-2 is smaller than that for ERS-1 at about -1.3 ms, again adopting the change of sign for the standard convention. The second order zonal coefficient, A_7, is now consistently negative but, more importantly, reveals little long-term variation. As for ERS-1, there is some evidence of an annual signal in A_3. For ERS-2 A_5 is the coefficient that exhibits long-term variability. This term corresponds to a North-South shift in the centre of figure and may be a consequence of the impact of PRARE correctly centring the ERS-2 altimetry in line with TOPEX/Poseidon. The final three values for A_5 may be anomalous but no conclusion can be drawn until cycle 34 becomes available.

The tandem period from May 1995 to June 1996 permitted a direct comparison of the ERS-1 and ERS-2 coefficients. A_3 - A_5 for both satellites reveal very similar trends given that the values are recovered over intervals of differing lengths. Similarly, A_7 follows similar trends although the ERS-2 values may be slightly more negative. Overall, the excellent correspondence confirms that the signals are real and affect both ERS satellites to the same extent. This is encouraging as we would expect the centre of figure of the ERS satellites to coincide as the tracking ought to be comparable. Similarly, the geophysical corrections are derived consistently and only the sea-state bias and wet tropospheric corrections are satellite dependent. The latter might account for small differences in the zonal term A_7.

Returning to the relative bias drift, Figure 13 re-plots the ERS-1 and ERS-2 relative bias with TOPEX. All DXO data was corrected for the observed trend in TOPEX as illustrated in Figure 10, the Gaussian solution. In this manner the ERS bias signatures are *independent* of the TOPEX bias trend. Figure 13 distinquishes between ERS-1 versions 3 and 6 as a clear discontinuity is observed due to the aforementioned incompatibilty of data before and after the start of the 2nd multidisciplinary phase. Overall, ERS-1 exhibits less variation than ERS-2. The results for ERS-1 and ERS-2 are presented in Tables 4 and 5 where the calendar date, bias values and standard deviations and numbers of DXO contributing to each bias value are presented. The formal accuracies are at the 1-2 mm level with higher SDs corresponding to the short time spans and the associated reduction in data.

Figure 11. Coefficients of Equation 6 for ERS-1.

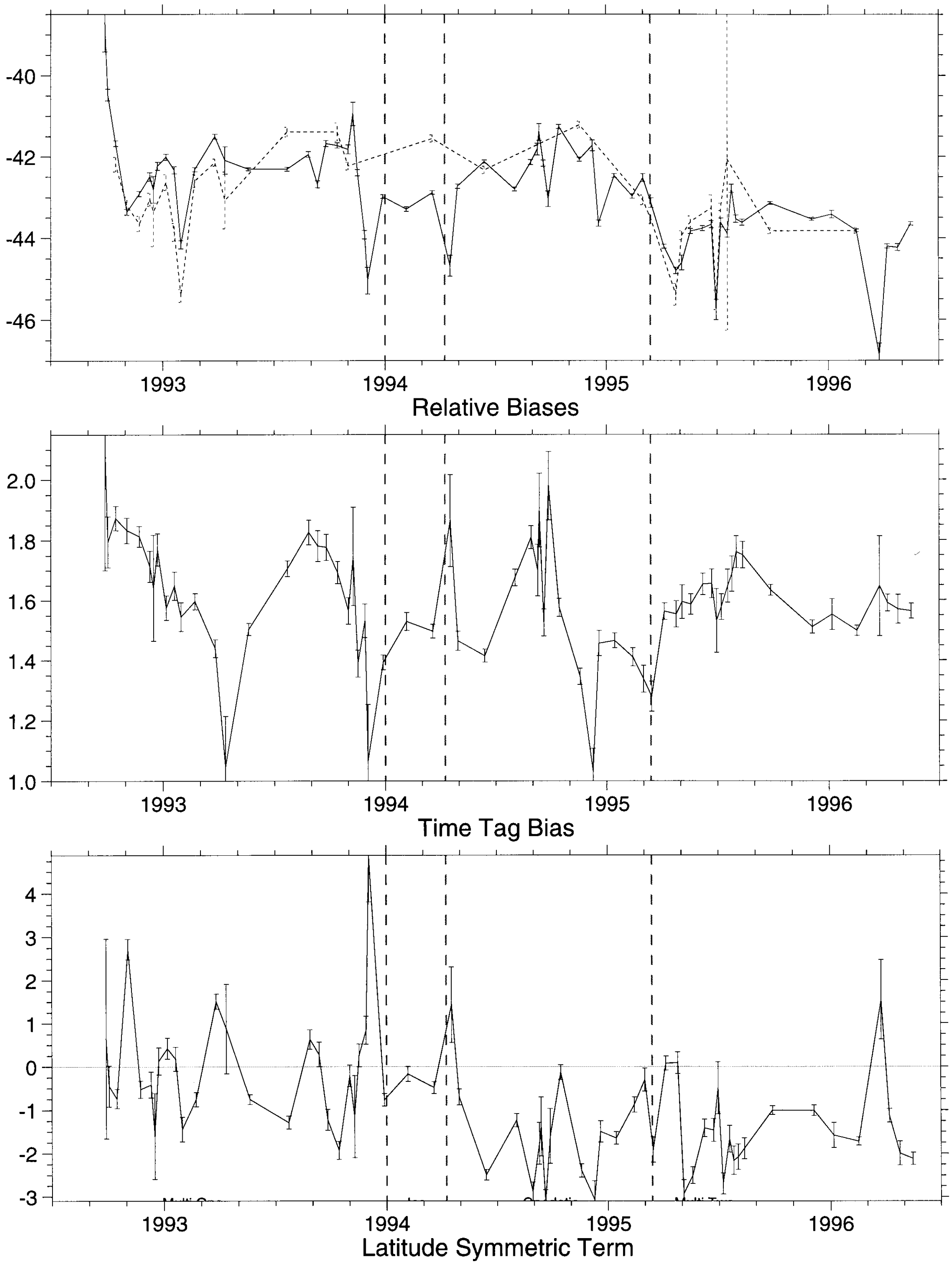

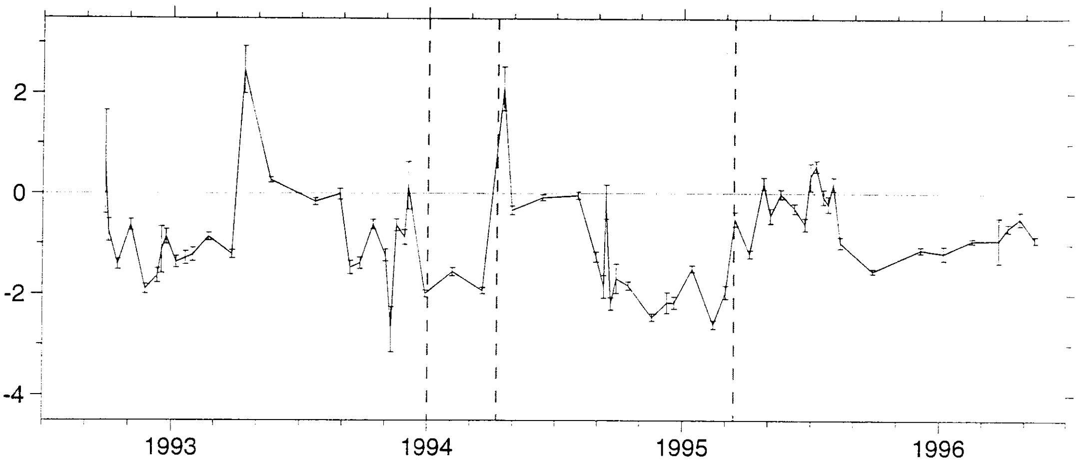
2
0
-2
-4
1993
1994
1995
1996

A3

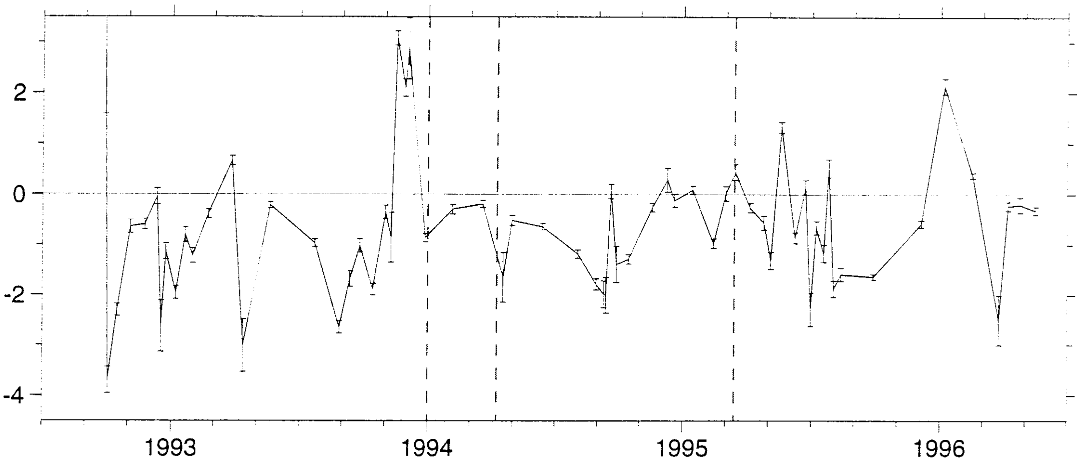
2
0
-2
-4
1993
1994
1995
1996

A4

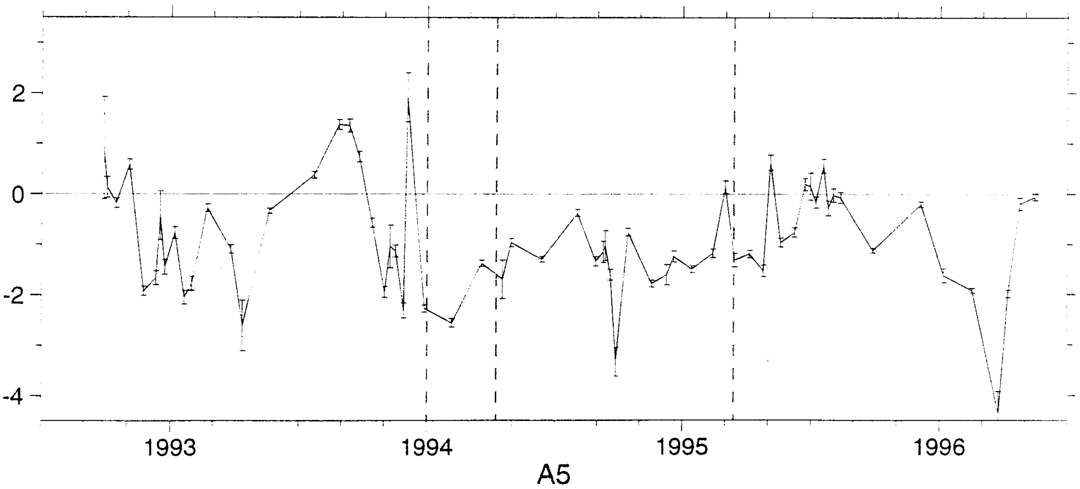
2
0
-2
-4
1993
1994
1995
1996

A5

Figure 12. Coefficients of Equation 6 for ERS-2.

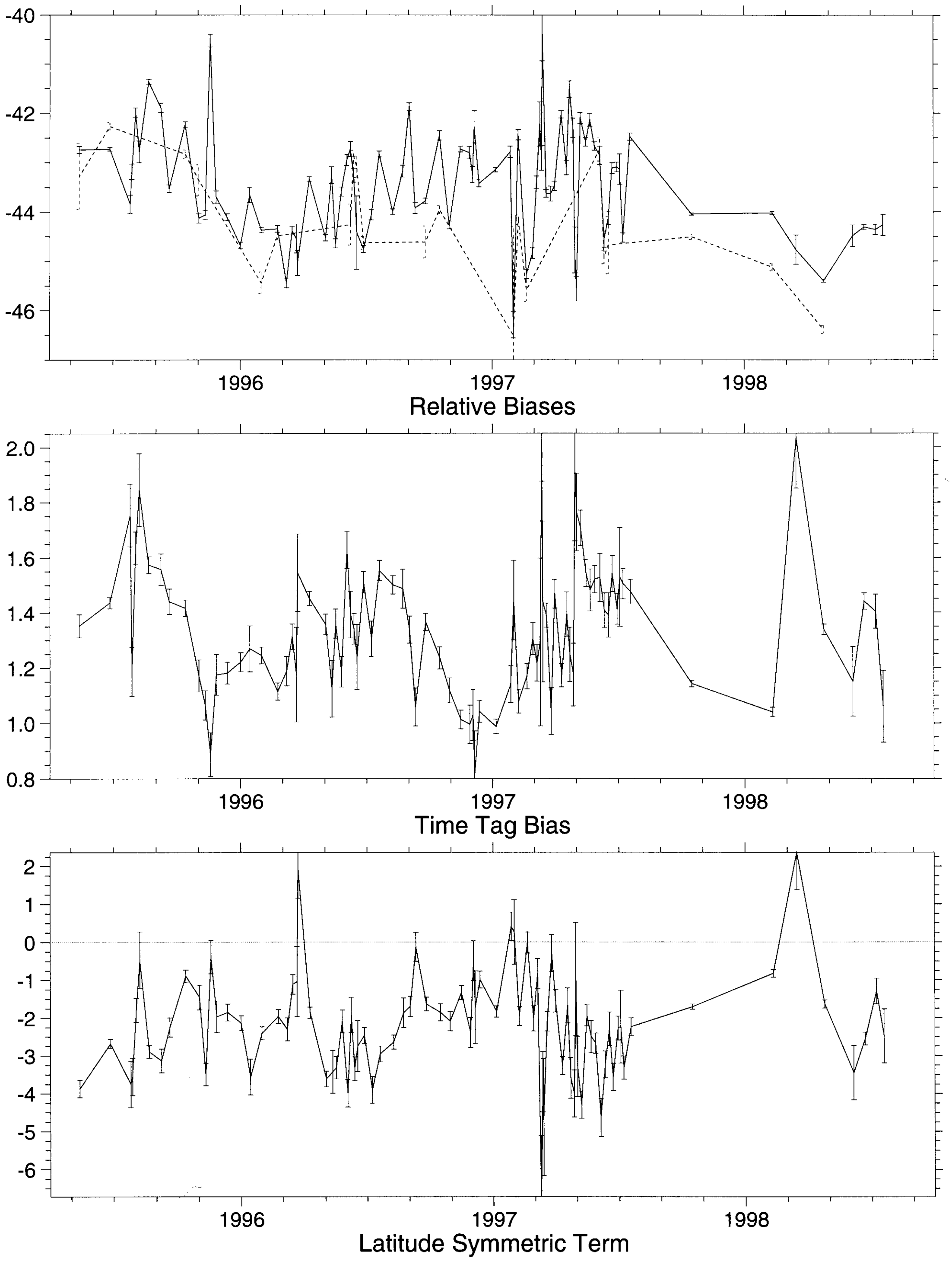

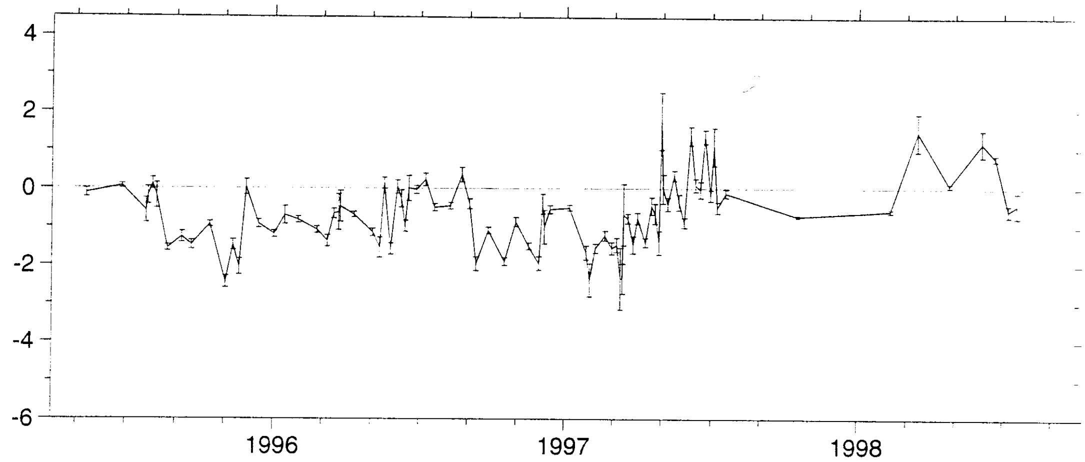
4
2
0
-2
-4
-6
1996
1997
1998
A3

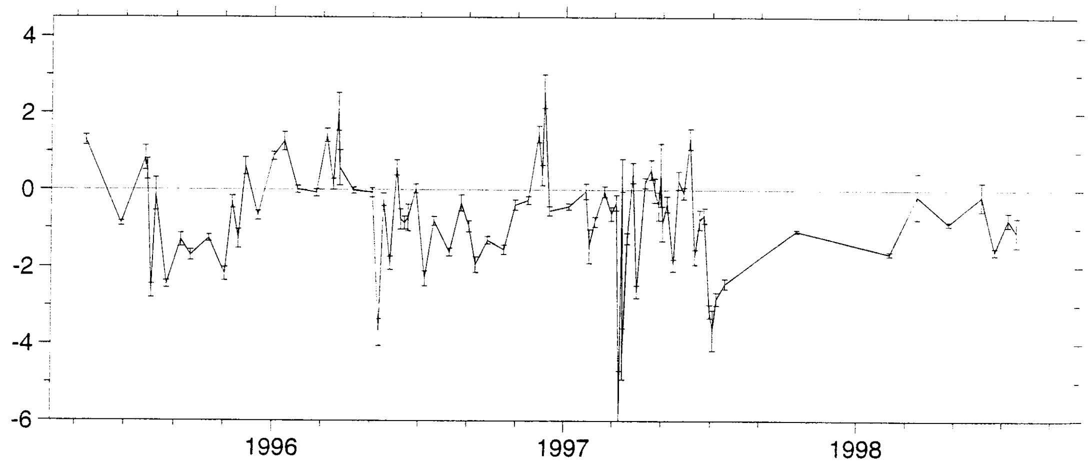
4
2
0
-2
-4
-6
1996
1997
1998
A4

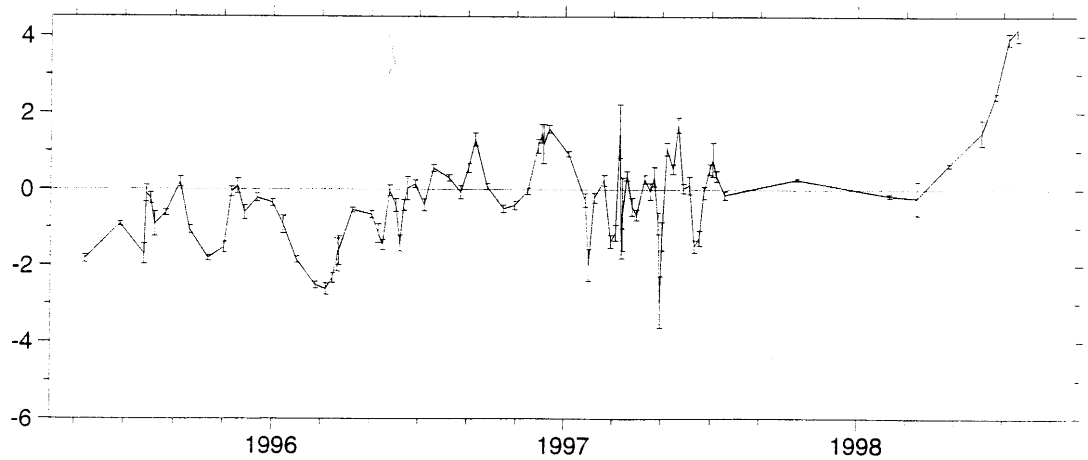
4
2
0
-2
-4
-6
1996
1997
1998
A5

Figure 13. ERS Bias Drift from DXO data

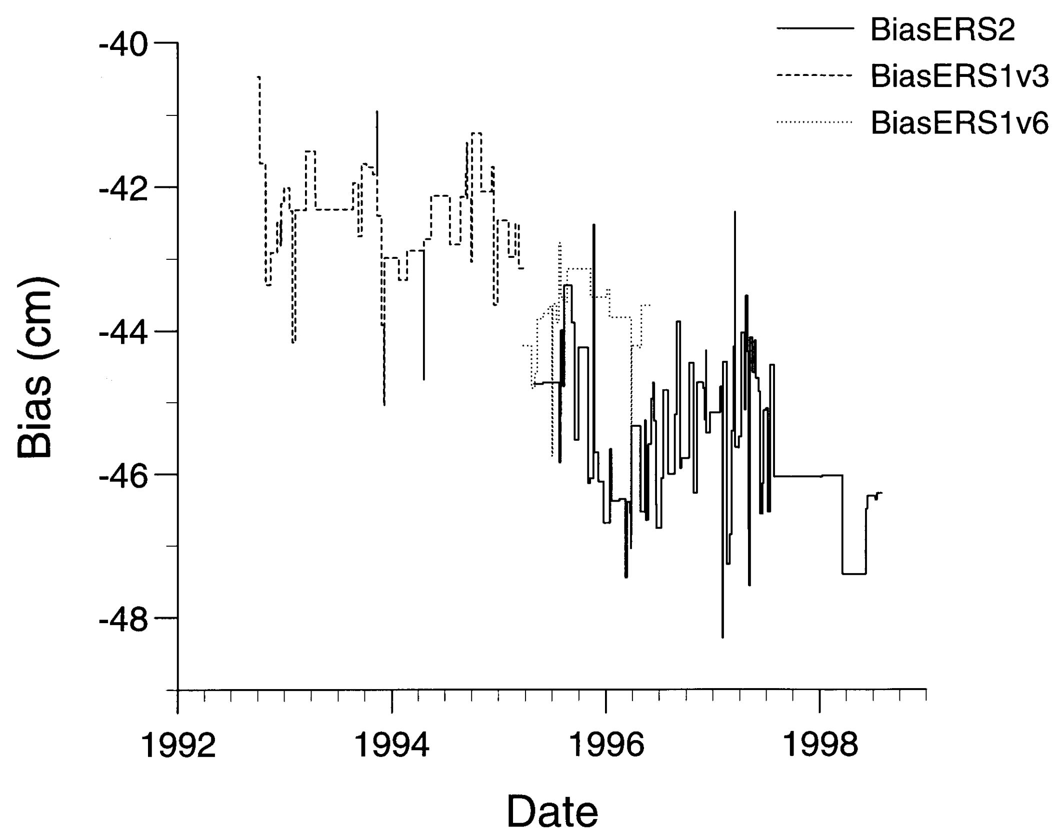

Date (yr,mth,day)	ERS-1 bias (cm)	sigma (cm)	# DXO
92 930 - 9210 7	-40.474	0.143	3981
9210 7 - 921026	-41.671	0.070	19169
921026 - 921112	-43.363	0.075	17197
921112 - 9212 6	-42.913	0.063	24132
9212 6 - 921216	-42.494	0.103	10544
921216 - 921218	-42.809	0.332	1334
921218 - 921229	-42.231	0.097	11670
921229 - 93 115	-42.009	0.079	18823
93 115 - 93 125	-42.330	0.092	11762
93 125 - 93 2 5	-44.162	0.100	12875
93 2 5 - 93 312	-42.320	0.051	40425
93 312 - 93 412	-41.505	0.062	36604
93 412 - 93 414	-42.093	0.340	1029
93 414 - 93 628	-42.308	0.035	77507
93 628 - 93 819	-42.309	0.048	41515
93 819 - 93 9 6	-41.945	0.069	16436
93 9 6 - 93 918	-42.682	0.087	10543
93 918 - 9310 4	-41.677	0.074	14511
9310 4 - 931025	-41.725	0.065	20440
931025 - 9311 9	-41.821	0.108	14490
9311 9 - 931110	-40.949	0.289	1085
931110 - 931124	-42.399	0.080	13581
931124 - 9312 3	-43.923	0.101	8698
9312 3 - 9312 4	-45.045	0.324	847
9312 4 - 94 122	-42.986	0.045	46510
94 122 - 94 220	-43.295	0.054	32649
94 220 - 94 418	-42.887	0.044	60199
94 418 - 94 419	-44.682	0.257	1173
94 419 - 94 513	-42.728	0.056	26656
94 513 - 94 717	-42.123	0.040	64084
94 717 - 94 821	-42.802	0.048	33268
94 821 - 94 9 8	-42.137	0.065	17004
94 9 8 - 94 912	-41.815	0.147	3371
94 912 - 94 914	-41.391	0.205	1739
94 914 - 94 926	-42.160	0.076	11594
94 926 - 94 930	-43.041	0.194	1970
94 930 - 941031	-41.257	0.051	29775
941031 - 9412 7	-42.065	0.052	33433
9412 7 - 941213	-41.721	0.136	4633
941213 - 941227	-43.641	0.075	14393
941227 - 95 2 2	-42.467	0.045	42514
95 2 2 - 95 225	-42.972	0.055	26682
95 225 - 95 3 9	-42.518	0.099	13033
95 3 9 - 95 324	-43.135	0.118	10823
95 324 - 95 421	-44.208	0.050	31372
95 421 - 95 5 2	-44.802	0.080	11974
95 5 2 - 95 510	-44.606	0.179	8365
95 510 - 95 531	-43.836	0.063	20881
95 531 - 95 618	-43.762	0.063	18626
95 618 - 95 630	-43.668	0.083	10453
95 630 - 95 7 3	-45.754	0.249	2115
95 7 3 - 95 716	-43.626	0.108	12743
95 716 - 95 724	-43.891	0.094	7765
95 724 - 95 730	-42.778	0.100	5884
95 730 - 95 8 7	-43.531	0.090	7946
95 8 7 - 95 820	-43.619	0.075	12159
95 820 - 9511 7	-43.142	0.033	72059
9511 7 - 96 1 3	-43.535	0.038	46871
96 1 3 - 96 111	-43.418	0.091	8490
96 111 - 96 325	-43.818	0.032	80683
96 325 - 96 326	-46.876	0.299	956
96 326 - 96 420	-44.206	0.049	28579

96 420 - 96 429	-44.235	0.084	9492
96 429 - 96 6 3	-43.647	0.043	36896

Table 4. ERS-1 relative bias (cm) and standard deviation (sigma) as recovered from DXO data with TOPEX (NRA). DXO residuals have been corrected for observed trend in the NRA.

Date (yr,mth,day)	ERS-2 bias (cm)	sigma (cm)	# DXO
95 429 - 95 531	-44.741	0.072	14124
95 531 - 95 726	-44.725	0.039	52633
95 726 - 95 728	-45.841	0.185	1925
95 728 - 95 731	-45.181	0.154	2508
95 731 - 95 8 8	-43.992	0.098	6857
95 8 8 - 95 810	-44.777	0.219	1412
95 810 - 95 9 4	-43.367	0.052	23148
95 9 4 - 95 914	-43.890	0.095	7629
95 914 - 95 928	-45.526	0.078	11702
95 928 - 951030	-44.234	0.060	27188
951030 - 9511 6	-46.127	0.103	6704
9511 6 - 951117	-46.064	0.090	8415
951117 - 951121	-42.525	0.132	3685
951121 - 9512 4	-45.701	0.128	4858
9512 4 - 951222	-46.107	0.069	14929
951222 - 96 112	-46.682	0.062	21088
96 112 - 96 118	-45.656	0.154	3645
96 118 - 96 214	-46.372	0.056	24335
96 214 - 96 3 5	-46.349	0.071	22504
96 3 5 - 96 311	-47.443	0.097	7013
96 311 - 96 321	-46.386	0.083	11110
96 321 - 96 323	-46.541	0.292	828
96 323 - 96 325	-47.040	0.255	1128
96 325 - 96 426	-45.330	0.045	34563
96 426 - 96 511	-46.529	0.065	15360
96 511 - 96 514	-45.254	0.169	2281
96 514 - 96 522	-46.643	0.091	7622
96 522 - 96 531	-45.587	0.093	7746
96 531 - 96 6 7	-44.950	0.114	5848
96 6 7 - 96 610	-44.726	0.149	2778
96 610 - 96 617	-45.259	0.138	7071
96 617 - 96 619	-46.425	0.746	1806
96 619 - 96 7 6	-46.758	0.073	15957
96 7 6 - 96 712	-46.058	0.107	5575
96 712 - 96 729	-44.828	0.063	16500
96 729 - 96 820	-45.998	0.057	20779
96 820 - 96 827	-45.172	0.119	4319
96 827 - 96 9 8	-43.875	0.082	10345
96 9 8 - 96 913	-45.921	0.115	4826
96 913 - 9610 8	-45.779	0.055	22767
9610 8 - 961024	-44.452	0.097	14144
961024 - 9611 5	-46.270	0.077	11149
9611 5 - 961126	-44.727	0.058	20139
961126 - 9612 1	-44.801	0.121	4401
9612 1 - 9612 5	-45.246	0.163	2390
9612 5 - 9612 6	-44.279	0.327	778
9612 6 - 961219	-45.423	0.069	13987
961219 - 97 123	-45.143	0.047	32669
97 123 - 97 131	-44.784	0.117	4977
97 131 - 97 2 1	-48.290	0.271	1178
97 2 1 - 97 214	-44.435	0.106	12746
97 214 - 97 225	-47.260	0.094	10402
97 225 - 97 3 3	-46.842	0.108	6776
97 3 3 - 97 3 9	-45.400	0.130	5351
97 3 9 - 97 313	-44.222	0.449	391
97 313 - 97 314	-44.903	0.256	1147
97 314 - 97 315	-42.347	0.593	306
97 315 - 97 325	-45.627	0.080	10910
97 325 - 97 328	-45.632	0.153	2997
97 328 - 97 4 5	-45.476	0.093	8749
97 4 5 - 97 417	-44.029	0.074	13047
97 417 - 97 420	-45.103	0.143	3494

97 420 - 97 426	-43.514	0.167	2647
97 426 - 97 430	-44.296	0.194	2081
97 430 - 97 5 1	-46.777	0.462	334
97 5 1 - 97 5 5	-47.561	0.248	1357
97 5 5 - 97 512	-44.098	0.112	5295
97 512 - 97 521	-44.584	0.086	9028
97 521 - 97 524	-44.136	0.133	3340
97 524 - 97 6 3	-44.665	0.084	9293
97 6 3 - 97 6 8	-44.852	0.184	3088
97 6 8 - 97 616	-46.556	0.163	5491
97 616 - 97 620	-46.129	0.139	3415
97 620 - 97 627	-45.113	0.111	6251
97 627 - 97 7 4	-45.087	0.097	6581
97 7 4 - 97 7 5	-45.136	0.309	718
97 7 5 - 97 713	-46.527	0.096	7233
97 713 - 97 726	-44.476	0.074	12142
97 726 - 98 1 7	-46.044	0.022	155837
98 1 7 - 98 316	-46.019	0.033	75258
98 316 - 98 317	-46.768	0.296	705
98 317 - 98 6 3	-47.398	0.034	70928
98 6 3 - 98 6 9	-46.489	0.224	1512
98 6 9 - 98 7 6	-46.310	0.051	25379
98 7 6 - 98 712	-46.361	0.105	5649
98 712 - 98 728	-46.267	0.218	1374

Table 5. ERS-2 relative bias (cm) and standard deviation (sigma) as recovered from DXO data with TOPEX (NRA). DXO residuals have been corrected for observed trend in the NRA.

8. ERS bias drift: Tide gauge results

In this section the bias drift in ERS altimetry is determined for all version 6 data, that is all ERS-2 cycles and ERS-1 cycles from the second multidisciplinary phase. It is important to recognise that the procedure used for TOPEX in section 6 cannot be applied to the ERS satellites due to the longer repeat pass period. For TOPEX the 4 ascending and descending passes closest to a tide gauge provide a maximum of 4 measurements every 10 days, a potential frequency of 1 measurement every 2.5 days. For ERS a similar strategy would yield 4 epochs every 35 days, a maximum frequency of 1 measurement every 8.75 days. Thus, to produce comparable data, the seven ascending and seven descending arcs closest to the gauge were employed giving 14 points every 35 days or 1 point every 2.5 days. In terms of longitudinal spread, the seven ERS arcs span 5.0° of longitude which compares well with the 5.3° span between the two TOPEX/Poseidon tracks.

Another crucial difference between TOPEX and ERS is the number of cycles available. In sections 5 and 6 a minimum of 140 cycles was deemed necessary for a repeat pass location to be accepted, the number providing a large statistical sample to derive the mean sea-level height at that location. The 33 cycles of ERS-2 to date do not yield sufficient data for the mean sea-level height to be inferred by simple averaging. The same conclusion holds even if ERS-2 is augmented with the 12 ERS-1 cycles of the second multidisciplinary phase. Of course as ERS-1 and ERS-2 have common ground tracks the mean sea-level height at common points along that ground track are pertinent to both ERS satellites. Even so, a total of 45 is still considered too low particularly as this is the maximum value when no data is missing. Even if the Ist ERS-1 multidisciplinary phase was added the maximum number would be 62 or 63. Thus a different approach is adopted in which the mean sea-surface heights are recovered simultaneously with the bias drift in a procedure which does not in effect assume that the mean value can be estimated a priori.

Given the above strategy ERS altimetric heights were determined at the nearest quarter degree of latitude to each of the 79 tide gauges accepted in section 5. As seen in Figure 8 several gauges were either inoperational or spasmodically operational during 1995 - 1998 reducing the tide gauges utilised to 75. The ERS altimetric measurements were subsequently corrected for the long wavelength spatial coefficients A_3 - A_5 and A_7 and the time tag error $A_6 r_\tau$ of section 7. These corrections, deduced from DXO data with epochs differing by 5 days or less, have been observed independently within the ERS data. As for dual crossover data the ERS altimetric bias was recovered as a step function constant between consecutive SPTR events. The bias was estimated in a simultaneous solution with the 641 geoid heights. Unlike TOPEX, where a zero mean for each repeat pass time series conditioned the solution, it is now not possible to separate the geoid heights from the bias drift. To overcome this deficiency the solution was conditioned by arbitrarily fixing one bias value. It is for this reason that the tide gauge solution for ERS gives the bias drift centred near zero rather than values close to the expected absolute bias.

The combined ERS-1 (version 6) and ERS-2 data comprised

- 6806 ERS-1 tide gauge enhanced measurements
- 16584 ERS-2 tide gauge enhanced measurements

and was analysed for

- 641 mean sea-level heights corresponding to the distinct repeat pass locations from 75 tide gauges
- 23 ERS-1 bias values
- 86 ERS-2 bias value with the system conditioned by fixing the value for the protracted period 17 Mar 1998 - 3 June 1998 (i.e. the largest interval between consecutive SPTR events).

As for the DXO data a rejection criterion of 25 cm was applied. The mean sea-level heights are of little interest per se except to note that the associated standard errors were generally 1.3-1.5 cm. A plot of the ERS bias solution is presented as Figure 14 with the values given in Tables 6 and 7. Note that the standard deviations for the tide gauge solutions are considerably larger than the DXO solutions in Tables 4 and 5. This is a direct response to the reduction in the quantity of data in the tide gauge solution with some periods having only a few tens of data points. The formal errors are generally at the sub centimetre level for intervals containing 100 or more tide gauge measurements but increase rapidly with the decrease in number. For intervals containing less than say 50 tide gauge measurements the formal errors render the bias value unreliable.

Figure 14. ERS Bias Drift from Tide Gauge Data

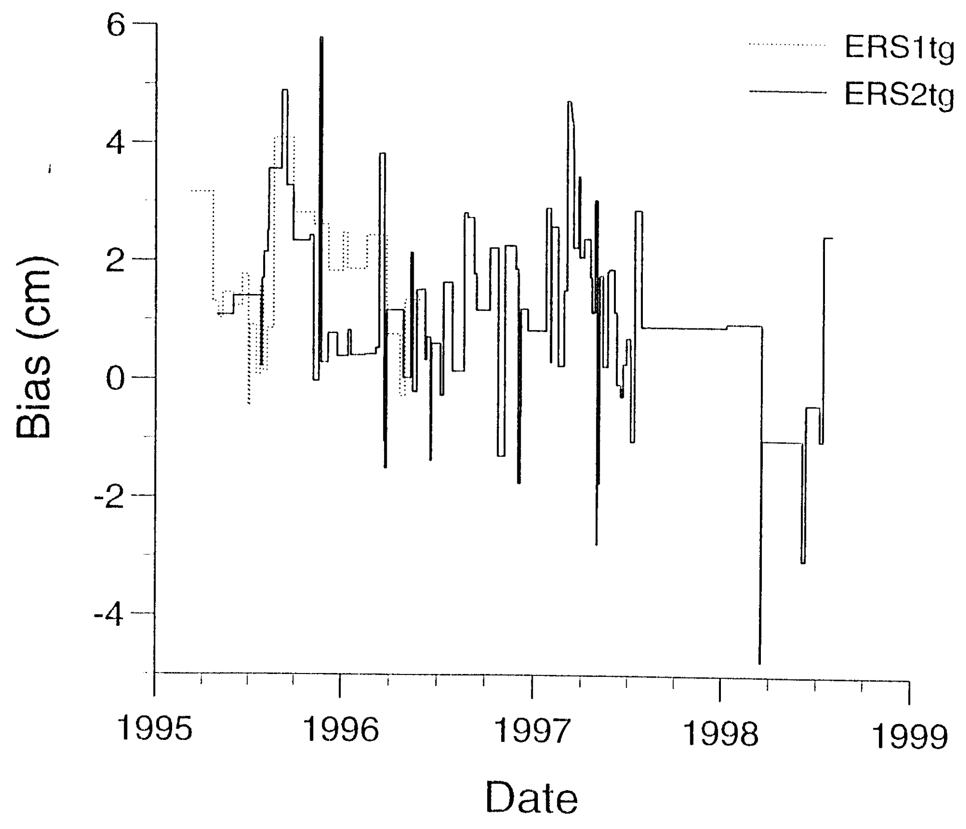

Date (yr,mth,day)	ERS-1 bias (cm)	sigma (cm)	# TG enhanced altimetry
95 3 9 - 95 421	3.164	0.489	436
95 421 - 95 5 2	1.308	0.698	179
95 5 2 - 95 510	1.023	0.815	125
95 510 - 95 531	1.463	0.546	338
95 531 - 95 618	1.242	0.567	296
95 618 - 95 630	1.760	0.718	169
95 630 - 95 7 3	-0.445	1.405	39
95 7 3 - 95 716	0.910	0.670	198
95 716 - 95 724	0.080	0.781	138
95 724 - 95 730	1.590	0.894	101
95 730 - 95 8 7	0.134	0.813	127
95 8 7 - 95 820	0.856	0.667	203
95 820 - 95 928	4.092	0.443	599
95 928 - 9511 7	2.813	0.439	613
9511 7 - 9512 5	2.612	0.493	427
9512 5 - 96 1 3	1.830	0.478	477
96 1 3 - 96 111	2.477	0.798	130
96 111 - 96 217	1.860	0.446	579
96 217 - 96 325	2.436	0.452	558
96 325 - 96 326	1.247	2.370	14
96 326 - 96 420	0.759	0.521	372
96 420 - 96 429	-0.284	0.779	143
96 429 - 96 6 3	1.341	0.455	545

Table 6 ERS-1 relative bias (cm) and standard deviation (sigma) as recovered from tide gauge enhanced altimetry corrected for coefficients A3 - A7 of Equation 6.

Date (yr,mth,day)	ERS-2 bias (cm)	sigma (cm)	# TG enhanced altimetry
95 429 - 95 531	1.083	0.631	237
95 531 - 95 726	1.401	0.395	881
95 726 - 95 728	0.224	1.577	30
95 728 - 95 731	1.696	1.271	47
95 731 - 95 8 8	2.144	0.858	113
95 8 8 - 95 810	2.514	1.686	27
95 810 - 95 9 4	3.560	0.508	406
95 9 4 - 95 914	4.892	0.804	130
95 914 - 95 928	3.284	0.659	206
95 928 - 951030	2.340	0.481	463
951030 - 9511 6	2.435	0.847	119
9511 6 - 951117	-0.027	0.749	160
951117 - 951121	5.787	1.141	65
951121 - 9512 4	0.284	0.676	190
9512 4 - 951222	0.774	0.572	290
951222 - 96 112	0.391	0.552	317
96 112 - 96 118	0.824	1.199	56
96 118 - 96 214	0.406	0.523	367
96 214 - 96 3 5	0.420	0.567	300
96 3 5 - 96 311	0.532	0.950	95
96 311 - 96 321	3.817	0.768	143
96 321 - 96 323	-1.037	2.136	16
96 323 - 96 325	-1.494	2.213	15
96 325 - 96 426	1.162	0.476	476
96 426 - 96 511	0.026	0.643	222
96 511 - 96 514	2.135	1.441	37
96 514 - 96 522	-0.205	0.860	110
96 522 - 96 531	1.508	0.812	125
96 531 - 96 6 7	1.514	0.910	98
96 6 7 - 96 610	0.335	1.371	42
96 610 - 96 617	0.709	0.917	97
96 617 - 96 619	-1.368	1.626	29
96 619 - 96 7 6	0.605	0.610	247
96 7 6 - 96 712	-0.261	0.915	96
96 712 - 96 729	1.628	0.591	270
96 729 - 96 820	0.133	0.532	347
96 820 - 96 827	2.819	1.044	73
96 827 - 96 9 8	2.734	0.710	173
96 9 8 - 96 913	1.775	0.958	88
96 913 - 9610 8	1.163	0.512	399
9610 8 - 961024	2.220	0.618	244
961024 - 9611 5	-1.295	0.697	179
9611 5 - 961126	2.264	0.567	302
961126 - 9612 1	1.859	1.108	66
9612 1 - 9612 5	-1.747	1.482	34
9612 5 - 9612 6	-0.610	2.699	10
9612 6 - 961219	1.194	0.684	194
961219 - 97 123	0.820	0.465	516
97 123 - 97 131	2.908	0.827	120
97 131 - 97 2 1	0.296	2.372	13
97 2 1 - 97 214	2.585	0.714	174
97 214 - 97 225	0.236	0.783	141
97 225 - 97 3 3	1.510	1.007	77
97 3 3 - 97 3 9	4.731	1.055	98
97 313 - 97 314	4.387	1.966	21
97 314 - 97 315	3.937	3.801	5
97 315 - 97 325	2.236	0.788	137
97 325 - 97 328	3.445	1.307	45
97 328 - 97 4 5	2.075	0.888	106
97 4 5 - 97 417	2.381	0.735	165
97 417 - 97 420	1.726	1.282	46
97 420 - 97 426	1.142	1.549	33

97 426 - 97 430	3.046	1.280	49
97 430 - 97 5 1	-2.777	2.287	14
97 5 1 - 97 5 5	-1.746	1.229	55
97 5 5 - 97 512	1.757	0.946	92
97 512 - 97 521	0.230	0.777	144
97 521 - 97 524	1.830	1.210	54
97 524 - 97 6 3	1.857	0.777	144
97 6 3 - 97 6 8	1.138	1.010	82
97 6 8 - 97 616	-0.073	0.884	103
97 616 - 97 620	-0.273	1.070	70
97 620 - 97 627	0.266	0.885	105
97 627 - 97 7 4	0.697	0.937	96
97 7 4 - 97 7 5	0.391	3.805	5
97 7 5 - 97 713	-1.029	0.794	135
97 713 - 97 726	2.872	0.689	181
97 726 - 98 1 7	0.900	0.323	2383
98 1 7 - 98 316	0.957	0.387	968
98 316 - 98 317	-4.749	2.837	9
98 317 - 98 6 3	-1.000		1000
98 6 3 - 98 6 9	-3.037	1.719	25
98 6 9 - 98 7 6	-0.395	0.530	356
98 7 6 - 98 712	-1.011	0.911	99
98 712 - 98 728	2.461	1.724	28

Table 7. ERS-2 relative bias (cm) and standard deviation (sigma) as recovered from tide gauge enhanced altimetry corrected for coefficients A3 - A7 of Equation 6.

9. Comparison of DXO and Tide Gauge Solutions

Two independent solutions of the ERS-2 bias drift have been determined from tide gauge and DXO data sets. A comparison of the solutions has been performed by adjusting the tide gauge solution to ‘best fit’ the DXO solution. Figure 15 presents such a comparison. Statistically, on removing outliers where the agreement exceeded 3.0 cm, the rms. difference is 0.81 cm with a correlation coefficient of 0.75. An alternative representation of the agreement is plotted in Figure 16 which shows the difference between the drift solutions centred on zero. In general, agreement is excellent during relatively large intervals between SPTR events. However, the spikes testify to the tide gauge methodology in particular being unable to monitor the drift over intervals of a few days. This is clearly evident around April 1997 where a rapid sequence of SPTR events corresponds to large formal errors in the tide gauge solution of Table 7.

Figure 15. ERS-2 Bias Drift Comparison: DXO and Tide Gauge Solutions

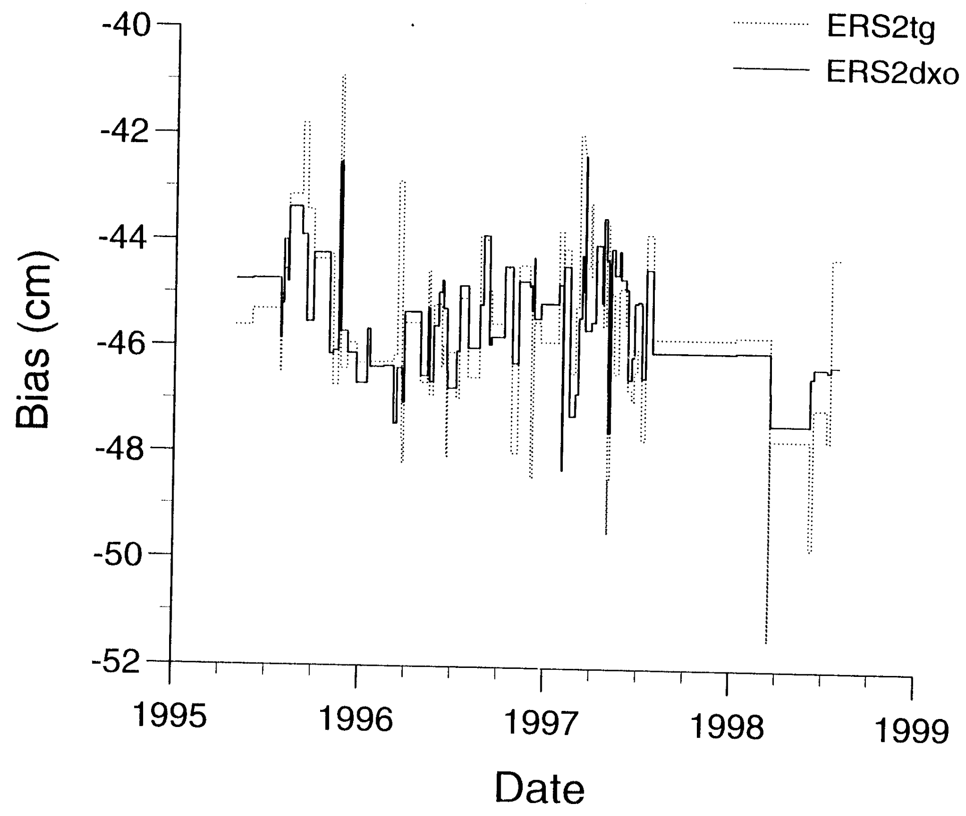

Figure 16. Difference between ERS-2 DXO and Tide Gauge Solutions

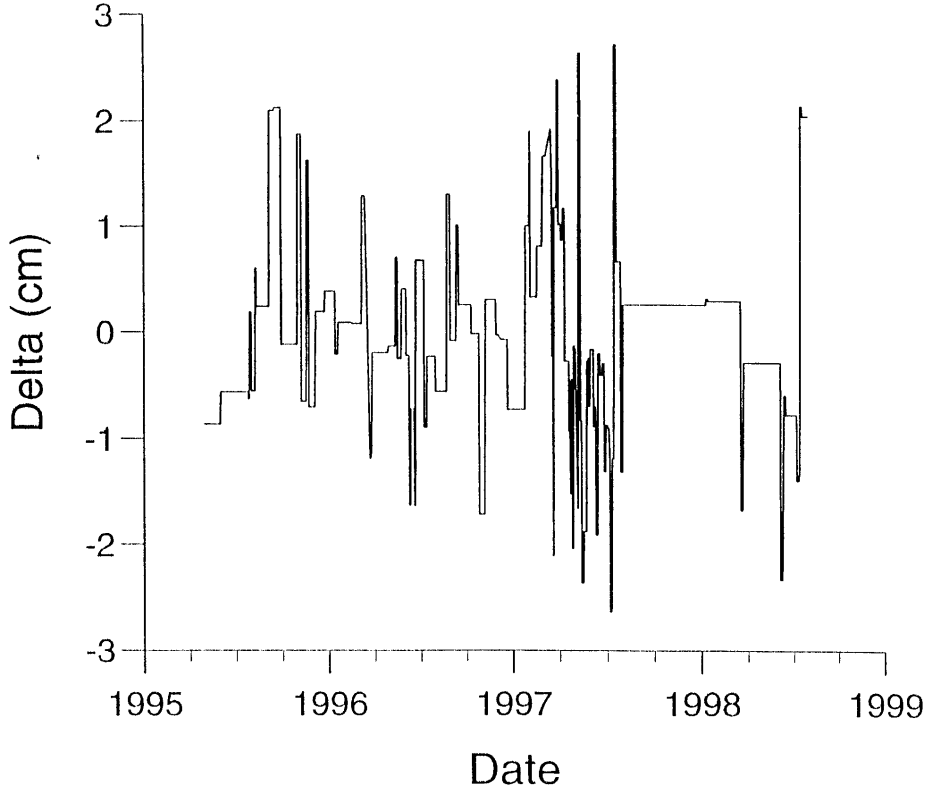

10. Conclusions and Recommendations

Preliminary studies of ERS-2 have revealed anomalous behaviour with respect to both ERS-1 and TOPEX/Poseidon. The objective of this study was to monitor the ERS-2 drift by two contrasting methodologies that are interwoven to some extent.

The methodology based on DXO residuals with TOPEX/Poseidon requires, as a prerequisite, comprehensive knowledge of the behaviour of the NRA altimetric range. Stability analysis of NRA has thus been undertaken by comparison against in situ data in the form of the global network of tide gauges in the FASTWOCE data set. After careful validation that the tide gauge was representative of the ocean response as measured by the altimeter, and elimination of some gauges which reveal evidence of excessive slope, a subset of 79 gauges was selected for further consideration. Utilising these gauges the ocean variability was removed from passes adjacent to each gauge enabling examination of residual signatures. Two methods were employed namely a step function constant over each TOPEX cycle and a smoother Gaussian weighting to monitor the NRA drift.

DXO data with ERS-1 and ERS-2 now enabled the relative bias drift of both ERS satellites to be extracted. The analysis removed the observed NRA drift and solved for other corrections such as the ERS time tag bias, displacements in the ERS centre of figure relative to TOPEX and an empirical second order zonal coefficient to absorb differences between polar and equatorial latitudes. Bias drift values were adjusted for each interval spanning the time between the event epochs of the SPTR correction file.

The alternative approach for ERS is to use the tide gauge data directly in a procedure reminiscent of that employed for TOPEX/Poseidon. Certain adjustments to the methodology were made to compensate for the longer repeat pass period and the associated reduction in cycles. The tide gauge enhanced altimetry was also adjusted for the observed trends in ERS altimetry as inferred from the DXO study.

A comparison of the two methodologies and in particular a comparison of the characteristics of the ERS-1 and ERS-2 solutions warrants the following comments:

- Monitoring the stability of altimetric range data through comparison against in situ tide gauge data is effective when the time interval for the individual bias values is large enough to enclose sufficient passes near the gauges. TOPEX spans of 10 days, i.e. 170-190 tide gauge enhanced observations, yielded formal errors near 4mm. For comparable accuracy about 30 days of ERS tracking is required (see Tables 6 and 7). Utilising the SPTR events as epochs for the intervals was acceptable for ERS-1 but the frequency of events for ERS-2 drastically degraded the study.
- The use of Equation 6 to correct the tide gauge enhanced altimetry is based on the corrections being attributable to ERS. The time tag bias presents few problems as the results concur with those derived from SXO data. Similarly, the 1st order harmonics, which absorb differences between the altimetric centre of figures, are more likely to be due to ERS given the nature of the relative tracking. However, A_7, the coefficient of the symmetric second order zonal term may be a composite of several effects including the sea-state bias for both ERS and TOPEX; inconsistency in the radiometric measurements

between the high vapour regime at the equator and lower content at the poles; deficiencies in the ERS ionospheric correction modelling etc. In practice, given consistency in the values for A_7, this term will have little impact if the tide gauges in each interval have comparable latitudinal spread. However, this will not always be the case for ERS-2 when the numbers of measurements are so small.

- The DXO solution for ERS-2 suffers to a lesser extent from the data limitation problem over short time spans but does require that the NRA bias drift is known to high accuracy. It is for this reason that much effort was devoted to monitoring the NRA altimetric range stability, in terms of both the passes and gauges that were acceptable.
- Inclusion of ERS-1 within the study was required for several reasons. Firstly, ERS-1 added slightly to the number of repeat passes in the ERS tide gauge study. This gave more confidence to the estimation of mean sea-level values. Equally, its inclusion enabled a direct comparison of the two ERS satellites. As shown in Figure 13, ERS-1 has two distinct sets of drift values, with a discontinuity as the OPR processing changed between versions 3 and 6 at the start of the 2nd multidisciplinary phase. This is unfortunate and degrades ERS-1 for long-term studies that require consistency within the data. However both versions reveal that the ERS-1 bias drift is more stable than ERS-2 particularly during the tandem mission. The apparent secular drift of near 2 cm over the first year of ERS-2 was perhaps, with hindsight, fortuitous as it identified a deficiency that may have been overlooked otherwise.
- Tables 4 and 5 for the ERS bias drift as recovered from DXO data are to be preferred to tide gauge based solutions in Tables 6 and 7 for the above reasons. The tide gauge methodology is a powerful technique and indispensable for TOPEX/Poseidon but less applicable to ERS unless time intervals of 30 days or so are chosen.
- Tables 4 and 5 establish that the bias anomalies for ERS-2 are larger than those of ERS-1 which is consistent with the magnitudes of the ESRIN SPTR corrections plotted in Figures 3 and 5. The scope of the study did not enable investigation of the precise cause of the anomalous behaviour but it is clear that a rapidly changing time series of corrections is required for which the SPTR events must remain the most likely candidate.

As a consequence of the study we recommend that ESRIN (ESA) instigate the following:

- All ERS-1 altimetry should be reprocessed and released as version 6, say. Such an action will involve expenditure. However, the long-term benefits of a consistent and integrated ERS data set are obvious.
- Further studies of the SPTR characterisation should be implemented in an attempt to reconcile the observed bias drift.
- The correction file for ERS-1 and ERS-2 in Tables 4 and 5 should be made available to the altimetric community.

References

Boomkamp, H J,Combination of altimetry data from different satellite missions, PhD thesis, Aston University, 1999.

Carnochan, S, Orbit and altimetric corrections for the ERS satellites through analysis of single and dual satellite crossovers, PhD thesis, Aston University, 1997.

Francis, C J, The calibration of the ERS-1 radar altimeter. In *Proceedings of the First ERS-1 Symposium: Space at the Service of the Environment,* ESA SP-259, 381-393, 1993.

Christensen, E J et al., Calibration of TOPEX/Poseidon at Platform Harvest, J. Geophys. Res., 99, 24465-24485, 1994.

AVISO, AVISO/CALVAL synthesis report: TOPEX/Poseidon cycles 1 to 181, AVI-NT-011-315-CN, Edition 1.0, 1998

Haines, B J and Y E Bar-Sever, Monitoring the TOPEX microwave radiometer with GPS; Stability of columnar water vapor measurements, Geophys. Res. Lett., in press, 1998.

Marshall, J A et al, The temporal and spatial characteristics of TOPEX/Poseidon radial orbit error, J. Geophys. Res, 100, 25331-25352, 1995.

Moore, P et al, Investigation of the stability of the ERS-1 range bias through tide gauge augmented altimetry, submitted to J. Geophys. Res., 1999.

Nerem, R S et al., Improved determination of global mean sea-level variations using TOPEX/Poseidon, Geophys. Res. Lett., 24(11), 1331-1334, 1997.

Roca M and C R Francis, Identification and origin of on-board bias jumps. In *Minutes of RA and MWR 2 CWG (#9),* ESA-ESRIN, 1996.

Rosborough, G W, Satellite orbit pertirbations due to the geopotential, *CSR-86-1,* Center for Space Research, University of Texas at Austin, 1986.

Scharroo R and P Visser, Precise orbit determination and gravity field improvement for the ERS satellites, J. Geophys. Res., 103, 8113-8127, 1998.

Tapley, B D et al, The Joint Gravity Model 3, J. Geophys. Res., 101, 28029-28049, 1996.

Wagner, C A and J Klokocnik, Accuracy of the GEM-T2 geopotential from GEOSAT and ERS-1 crossover altimetry, J. Geophys. Res., 99, 9179-9201, 1994.